

**NASA
Technical
Paper
2793**

1988

A Study To Evaluate STS
Heads-Up Ascent Trajectory
Performance Employing a
Minimum-Hamiltonian
Optimization Strategy

Sujit Sinha

*George C. Marshall Space Flight Center
Marshall Space Flight Center, Alabama*



National Aeronautics
and Space Administration

Scientific and Technical
Information Division

ACKNOWLEDGMENTS

The author expresses his thanks and gratitude to those individuals who provided guidance and support during the course of this study. Special thanks to Dr. Frank C. Liu of the University of Alabama in Huntsville for his assistance in understanding trajectory dynamic principles and minimum-Hamiltonian optimization.

TABLE OF CONTENTS

	Page
I. INTRODUCTION	1
II. METHOD	1
A. Simulation Program	1
B. Optimization Methodology	4
C. Optimization Iteration Process	7
D. MASTRE Program Modifications	11
E. Trajectory Simulation Groundrules	12
F. Procedure	15
III. RESULTS	16
IV. DISCUSSION	34
V. CONCLUSIONS	37
REFERENCES	38
BIBLIOGRAPHY	39
APPENDIX — MASTRE NAMELIST INPUT EXAMPLE	41

LIST OF ILLUSTRATIONS

Figure	Title	Page
1.	Comparison of heads-up and heads-down attitudes.....	2
2.	Attitude angle definition	3
3.	Chord min-H geometry (H_u versus U at a fixed time T)	9
4.	Heads-up injection weight comparison	17
5.	SRM vacuum thrust comparison	23
6.	Heads-up versus heads-down SSME power level comparison	23
7.	Heads-up versus heads-down altitude comparison	25
8.	Heads-up versus heads-down range comparison	25
9.	Heads-up versus heads-down altitude/range comparison	26
10.	Heads-up versus heads-down relative velocity comparison	26
11.	Heads-up versus heads-down relative gamma comparison	27
12.	Heads-up versus heads-down alpha comparison	27
13.	Heads-up versus heads-down beta comparison	29
14.	Heads-up versus heads-down Mach number comparison	29
15.	Heads-up versus heads-down chi-pitch comparison	30
16.	Heads-up versus heads-down chi-yaw comparison.....	30
17.	Heads-up versus heads-down chi-roll comparison.....	32
18.	Heads-up versus heads-down Q comparison	32
19.	Heads-up versus heads-down $Q \cdot \alpha$ comparison	33
20.	Heads-up versus heads-down $Q \cdot \beta$ comparison	33
21.	Heads-up versus heads-down acceleration comparison	34

LIST OF TABLES

Table	Title	Page
1.	Heads-Up Performance/Trajectory Summary for Unconstrained Q	18
2.	Heads-Up Performance/Trajectory Summary, Q Constraint of 660 PSF	19
3.	Heads-Up Performance/Trajectory Summary, Q Constraint of 680 PSF	20
4.	Heads-Up Performance/Trajectory Summary, Q Constraint of 700 PSF	21
5.	Heads-Up Performance/Trajectory Summary, Q Constraint of 720 PSF	22

ACRONYMS AND SYMBOLS

α	Angle of attack
β	Angle of sideslip
γ_R	Relative flight path angle
λ	Lagrange multiplier
ν	Lagrange multiplier (constant)
ϕ	Payoff quantity
χ_P	Pitch attitude angle
χ_R	Roll attitude angle
χ_Y	Yaw attitude angle
ψ	Terminal or intermediate constraint
ASRM	Advanced Solid Rocket Motor
cg	Center of gravity
ET	External Tank
F	Total force
FWC	Filament Wound Case
G	Gravitational acceleration
GPC	General Purpose Computer
H	Hamiltonian
I-load	Initialization Load
Isp	Specific impulse
IVBC-3	Integrated Vehicle Baseline Configuration 3
LH ₂	Liquid hydrogen

LOX	Liquid oxygen
M	Total mass
MASTRE	Minimum Hamiltonian Ascent Shuttle Trajectory Evaluation
max-Q	Maximum dynamic pressure
MECO	Main Engine Cutoff
min-H	Minimum Hamiltonian
MPS	Main Propulsion System
MSFC	Marshall Space Flight Center
NASA	National Aeronautics and Space Administration
OMS	Orbital Maneuvering System
PMBT	Propellant Mean Bulk Temperature
PRM-4	Performance Reference Mission 4
Q	Dynamic pressure
$Q\alpha$	Product of dynamic pressure with angle of attack
$Q\beta$	Product of dynamic pressure with angle of sideslip
RAGMOP	Rocket Ascent G-Limited Moment Balance Optimization Program
R_b	Burnrate (@ 60°F and 625 psia)
RCS	Reaction Control System
ROBOT	Robert's Optimum Trajectory
RPL	Rated Power Level
RRA	Range Reference Atmosphere
SODS	Shuttle Operational Data Submittal
SRB	Solid Rocket Booster

SRM	Solid Rocket Motor
SSME	Space Shuttle Main Engine
STS	Space Transportation System
t	Time
TPS	Thermal Protection System
u_q	Control variable
VLS	Vandenberg Launch Site
V_R	Relative velocity
WTR	Western Test Range
X_K	Differentiated Variable
(\cdot)	Differentiated with respect to time
(\cdot)'	Matrix transpose

TECHNICAL PAPER

A STUDY TO EVALUATE STS HEADS-UP ASCENT TRAJECTORY PERFORMANCE EMPLOYING A MINIMUM-HAMILTONIAN OPTIMIZATION STRATEGY

I. INTRODUCTION

The Space Transportation System (STS), more commonly known as the Space Shuttle, is currently America's primary heavy-lift launch vehicle. Therefore, any vehicle performance enhancements are of significant interest. One method identified to potentially increase STS performance is to alter the trajectory of the vehicle such that it flies in a "heads-up" mode. The term heads-up refers to the relative position of a crew member in the shuttle with respect to the ground (Fig. 1).

The objective of this study is to ascertain the performance capability of the STS, as a function of Solid Rocket Motor (SRM) burnrate and maximum dynamic pressure (max Q), for heads-up flight. The results can then be compared to the current heads-down flight mode.

II. METHOD

A. Simulation Program

The program used to simulate shuttle ascent trajectories, in this study, is referred to as the Minimum Hamiltonian Ascent Shuttle Trajectory Evaluation (MASTRE) program. Development of this program was completed in November 1974 as an outgrowth of three NASA Marshall Space Flight Center (MSFC) programs: RAGMOP [1], ROBOT [2], and Lifting ROBOT [3]. Trajectory optimization is obtained by a steepest ascent algorithm using a minimum Hamiltonian (min-H) strategy, where the derivation has been expanded to encompass the effects of the atmosphere and of moment balance control. The combined effects of aerodynamics and fixed engine offsets are counterbalanced, or moment balanced, by controllable engines. Three degrees-of-freedom are maintained in the program by instantaneous command and response of the controllable engines; therefore, no vehicular angular rates are considered. Note, the controllable engines can be either the SRMs or the Space Shuttle Main Engines (SSMEs), but not both.

The pitch attitude angle (χ_P), yaw attitude angle (χ_Y), and roll attitude angle (χ_R) used in the MASTRE program are defined in Figure 2. The X_P , Y_P , and Z_P axes form an Earth-centered inertial plumbline coordinate system; where Y_P is the local vertical, X_P is directed along the flight azimuth, and Z_P forms a right-handed system. The body coordinate system is defined by X_m , Y_m , and Z_m axes; where Y_m is along the longitudinal axis of the vehicle, X_m points away from the orbiter tail, and Z_m forms a right-hand set. Therefore, χ_P is measured from the local vertical to the projection of the external tank centerline in the Y_P - X_P plane. Whereas, χ_Y is measured from the ET centerline to the projection of the ET centerline in the Y_P - X_P plane. Finally, χ_R is measured about the ET centerline.

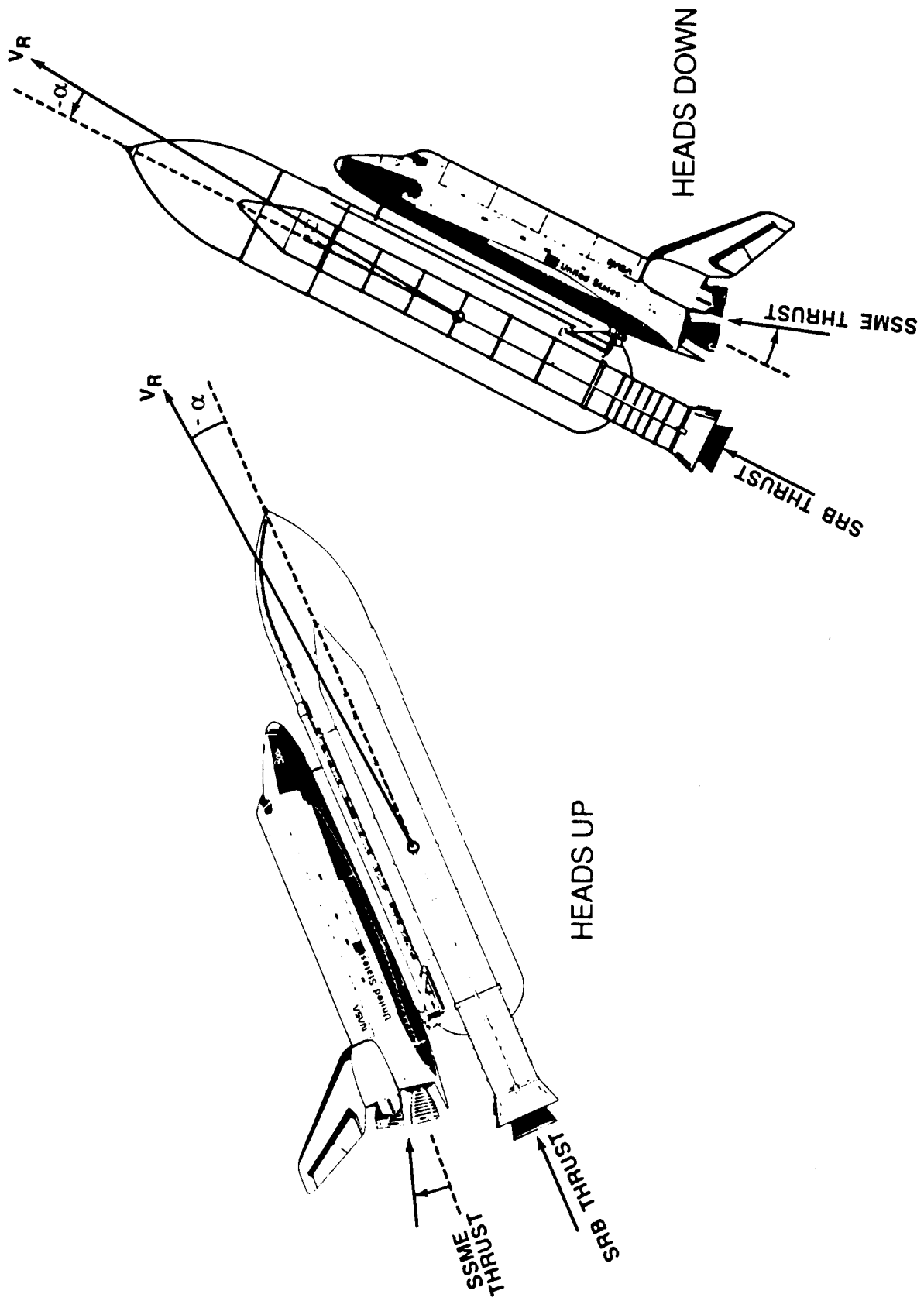


Figure 1. Comparison of heads-up and heads-down attitudes.

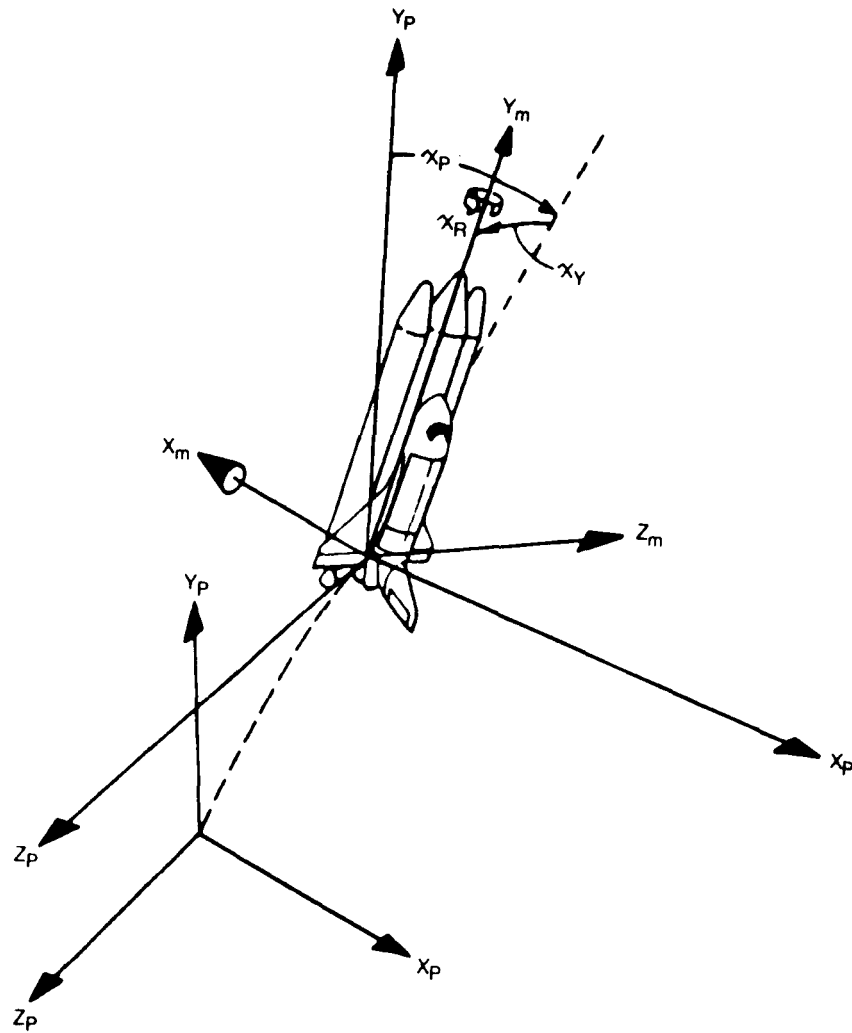


Figure 2. Attitude angle definition.

The gravitational model in the program is derived from the rotating Fischer Earth model, which establishes a "pear shaped," ellipsoidal Earth model. The model also serves as the reference for altitude computation. Details of this model are described in Reference 4.

The other models and/or groundrules used in this study are listed in the Groundrules section of this report. A description of the min-H optimization process used by the MASTRE program is presented in the next section.

B. Optimization Methodology

The trajectory optimization procedure employed in the MASTRE program is known as the Minimum Hamiltonian Method. A basic discussion of this optimization scheme follows.

Given, a set of n nonlinear differential equations

$$\dot{X}_i = f_i(u_\ell, X_K, t) \quad ; \quad i, k = 1 \rightarrow n \quad ; \quad \ell = 1 \rightarrow r \quad (2.1)$$

where

u_ℓ – control variable (not differentiated)

X_K – differentiated variable (one derivative only)

t – time .

In the MASTRE program, the nonlinear differential equations are the primary equations of motion. These equations are integrated using a fourth-order Runge-Kutta numerical integration scheme and are given by

$$\dot{X}_1 = \dot{W} = \frac{F_x}{M} + G_x \quad (2.2)$$

$$\dot{X}_2 = \dot{U} = \frac{F_y}{M} + G_y \quad (2.3)$$

$$\dot{X}_3 = \dot{V} = \frac{F_z}{M} + G_z \quad (2.4)$$

$$\dot{X}_4 = \dot{X} = W \quad (2.5)$$

$$\dot{X}_5 = \dot{Y} = U \quad (2.6)$$

$$\dot{X}_6 = \dot{Z} = V \quad (2.7)$$

$$\dot{X}_7 = -(\dot{m}_{SSME} + \dot{m}_{SRB}) \quad \} \quad \text{mass flow rates} \quad (2.8)$$

Where,

F – the total force on the vehicle due to thrust aerodynamics and winds

M – the total vehicle mass

G – the gravitational acceleration .

Note, equation (2.8) is not an equation of motion and does not require numerical methods for integration. The flow rates are input data and are shown to point out the source of vehicle mass changes.

Also,

SRM Thrusts – are obtained from user input sequential access files

SSME Thrusts – are tag values, which are input via the ENGDAT namelist variable (see Appendix)

Aerodynamic Forces – are determined by table look-up, as functions of Mach number, angle of attack (α), and angle of sideslip (β)

Wind Forces – are determined by table look-up as a function of altitude, and the wind month is input by the namelist variable IWNUM (see Appendix).

Now, rearranging the equations of motion, the following equation is established

$$y_i \equiv \dot{X}_i - f_i \quad , \quad i = 1 \rightarrow n \quad . \quad (2.9)$$

Then, the introduction of Lagrange multipliers leads to

$$E \equiv \lambda_i(t)y_i = \lambda_i(t) [\dot{X}_i - f_i] \quad , \quad i = 1 \rightarrow n \quad . \quad (2.10)$$

From calculus of variations, an integral can be minimized (or maximized) via the use of the Euler equation, which results in the following :

$$\frac{d}{dt} \left(\frac{\partial E}{\partial \dot{X}} \right) - \frac{\partial E}{\partial X} = 0 \quad , \quad (2.11)$$

which leads to,

$$\frac{d}{dt} \lambda_i + \sum_{K=1}^n \lambda_K \frac{\partial f_K}{\partial X_i} = 0, \quad i = 1 \rightarrow n \quad (2.12)$$

or,

$$\lambda_i + \sum_{K=1}^n \lambda_K \frac{\partial f_K}{\partial X_i} = 0, \quad i = 1 \rightarrow n \quad (2.13)$$

and, in matrix form

$$\dot{\lambda} = - \left(\frac{\partial f}{\partial X} \right) \lambda \quad (2.14)$$

This equation is known as the adjoint equation.

Also,

$$\frac{d}{dt} \frac{\partial E}{\partial \dot{u}} - \frac{\partial E}{\partial u} = 0, \quad (2.15)$$

which yields,

$$\sum_{K=1}^n \lambda_K \frac{\partial f_K}{\partial u_\ell} = 0, \quad \ell = 1 \rightarrow r \quad (2.16)$$

where,

$$\left(\frac{\partial E}{\partial \dot{u}} \right)' = 0 \quad (2.17)$$

So, in matrix form

$$\left(\frac{\partial f}{\partial u} \right)' \lambda = 0 \quad (2.18)$$

or,

$$\left(\frac{\partial H}{\partial u}\right)' = H_u = 0 \quad (2.19)$$

where, $H = f'\lambda$ is known as the Hamiltonian. The above equation is an $\ell \times 1$ matrix of the partial derivatives of the Hamiltonian with respect to control variables, and is the optimality equation. MASTRE program control variables used in this study include χ_P , χ_Y , main engine cutoff (MECO) time, and SSME throttle down to 65 percent initiation time during first stage.

Initial conditions must be satisfied in the solution process, and these conditions are given by

$$X_i(t_0) = X_{0i}, \quad i = 1 \rightarrow n \quad (2.20)$$

These variables include initial vehicle position, velocity, acceleration, and mass.

Also, the P terminal or intermediate constraints have to be satisfied. These constraints are given by

$$\psi_j = \psi_j [X(t), t], \quad j = 1 \rightarrow P \quad (2.21)$$

where,

$$t = \begin{cases} t_{\text{MECO}}, & \text{for terminal constraints} \\ t_i, & \text{for intermediate constraints} \end{cases}$$

The terminal constraints are MECO targeting conditions, which include altitude, velocity, and flight path angle. In the case of intermediate constraints, time is no longer MECO time but some intermediate time. Intermediate constraints used in this study are vehicle dynamic pressure and vehicle longitudinal acceleration.

Now, while satisfying all of the previous conditions, a payoff quantity is to be minimized or maximized. This quantity is given by

$$\phi = \phi[X(t_{\text{MECO}}), t_{\text{MECO}}] \quad (2.22)$$

In this study the payoff quantity is the MECO or injection weight, and this parameter requires maximization to achieve maximum performance.

Note, the Lagrange multipliers used in the adjoint and optimality equations are given by

$$\lambda(t) = \lambda_{\phi}(t) + \lambda_{\psi}(t) \nu \quad (2.23)$$

where

λ – is a nx1 matrix

λ_{ϕ} – is a nx1 matrix

λ_{ψ} – is a nxP matrix

ν – is a Px1 matrix and consists of constant Lagrange multipliers associated with the terminal or intermediate constraints

and,

$$\lambda_{\phi} = \left[\frac{\partial \phi}{\partial X} \right]' \quad (2.24)$$

which is evaluated at $t = t_{meco}$

$$\lambda_{\psi} = \left[\frac{\partial \psi}{\partial X} \right] \quad (2.25)$$

which is evaluated at

$$t = \begin{cases} t_{MECO}, & \text{for terminal constraints} \\ t_i, & \text{for intermediate constraints} \end{cases}$$

The above equations are obtained by using the transversality conditions, and again they allow for the determination of the Lagrange multipliers at the terminal and/or intermediate time.

C. Optimization Iteration Process

For optimum conditions, as shown in equation (2.19), $H_u = 0$. However, in general this relation will not be true for initially chosen values of the control parameter, $u(t)$, and the Lagrange multipliers associated with the terminal or intermediate constraints, ν . Therefore, in order to satisfy the optimality equation (2.19), initial conditions (2.20) and terminal/intermediate constraints (2.21), an iterative solution process is necessary.

The first step in this procedure involves the selection of initial values for the control parameters (χ_P , χ_Y , MECO time, and SSME throttle down to 65 percent initiation time during first stage) and the Lagrange multipliers associated with the terminal or intermediate constraints. The optimization method generates changes to these initial values, and this process is described by

$${}^{(i+1)}u(t) = {}^i u(t) + \delta u(t) \quad (2.26)$$

and

$${}^{(i+1)}v = {}^i v + dv \quad (2.27)$$

where,

i – is a superscript representing the i^{th} iteration

$(i+1)$ – is a superscript representing the $(i^{\text{th}} + 1)$ iteration

$\delta u(t)$ and dv – are zero for the 0^{th} iteration.

Now, knowing the above values, a forward integration of the n nonlinear differential equations (2.1) occurs from $X(t_0) = X_0$ to the currently established MECO time. Next, the adjoint equation (2.14) is integrated backwards from the known MECO time to t_0 , in order to calculate the Lagrange multipliers. Note, since the MECO time is known, the initial value of λ is obtained from equation (2.23), where $t = t_{\text{MECO}}$. Also, during each step of the backward integration of the adjoint equation, the value of the optimality equation is calculated from

$$H_u = \left(\frac{\partial f}{\partial u} \right)' \lambda \quad , \quad (2.28)$$

which is a combination of equations (2.18) and (2.19), and for optimum conditions $H_u = 0$. Recall, in general the above equation will not be zero for the initially chosen $u(t)$ and v . Therefore, to force H_u to zero, changes need to be made to the control parameters, $u(t)$, and the effect these changes have on the constraints need to be accounted for by also changing the Lagrange multipliers associated with the constraints, v .

From "chord min-H" geometry shown in Figure 3, the following equations are used to generate the necessary changes to drive H_u to zero.

$$\delta u = -(u^* - u_c)P + H_{uu}^{-1} G' \lambda_\psi I_{\psi\psi}^{-1} [d\psi + I_{\psi c} P] \quad (2.29)$$

and,

$$dv = -I_{\psi\psi}^{-1} (I_{\psi c} P + d\psi) \quad (2.30)$$

where

$$G' \lambda_\psi = H_{u\lambda} \left(\frac{\partial \lambda}{\partial v} \right) = \left(\frac{\partial f}{\partial u} \right)' \lambda \quad (2.31)$$

$$I_{\psi\psi} = \int_{t_0}^{t_{MECO}} \lambda'_\psi G H_{uu}^{-1} G' \lambda_\psi dt \quad (2.32)$$

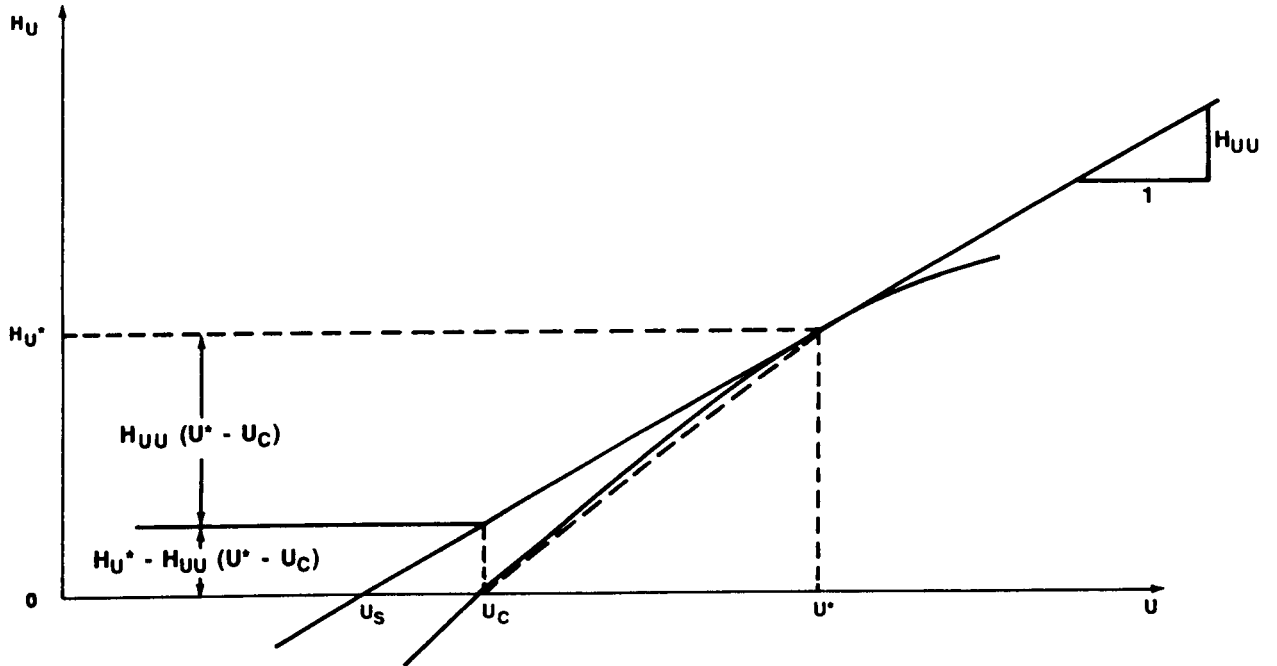


Figure 3. Chord min-H geometry (H_u versus U at a fixed time t).

$$I_{\psi c} = \int_{t_0}^{t_{MECO}} \lambda'_{\psi} G(u^* - u_C) dt \quad (2.33)$$

and

$$P = \left(\frac{dP^2 - d\psi' I_{\psi\psi}^{-1} d\psi}{I_{CC} - I_{\psi c} I_{\psi\psi}^{-1} I_{\psi c}} \right)^{1/2} \quad (2.34)$$

Now,

$$dP^2 = \int_{t_0}^{t_{MECO}} \delta u' H_{uu} \delta u dt \quad (2.35)$$

and

$$I_{CC} = \int_{t_0}^{t_{MECO}} (u^* - u_C)' H_{uu} (u^* - u_C) dt \quad (2.36)$$

The strategy involved in determining $\delta u(t)$ and $d\nu$ is to first select a value for dP^2 and set $d\psi = -\psi$. Now, for

$$dP^2 - d\psi' I_{\psi\psi} d\psi < 0$$

then set $P = 0$ and $d\psi = -K\psi$, where

$$K = \left(\frac{dP^2}{d\psi' I_{\psi\psi}^{-1} d\psi} \right)^{1/2} \quad (2.37)$$

or for

$$dP^2 - d\psi' I_{\psi\psi} d\psi \geq 0$$

then set $P = 1$ or to the calculated P , whichever is the smaller value. Once $P = 1$, discontinue the use of dP^2 to calculate P .

Hence, with $\delta u(t)$ and $d\nu$ known, the iteration procedure is repeated until the optimality equation, initial conditions, and the constraints are satisfied within some tolerance.

The process just described is again referred to as chord min-H and is a convergence scheme designed for use with high-speed digital computers. Further information on the chord min-H formulation is described in Reference 5.

D. MASTRE Program Modifications

As stated in the introduction, the purpose of this study is to examine the performance implications of heads-up shuttle ascent. However, previous trade studies conducted by Rockwell International [6] indicate that rolling the vehicle to heads-down, from an initially heads-up ascent, prior to Solid Rocket Booster (SRB) separation increases STS performance. This performance increase occurs because if a heads-up profile is maintained during staging, thrust from the SSMEs (which provide trim control during SRM thrust tailoff and after staging) is forced to a non-optimum angle. The non-optimum condition is a result of angle of attack (α) constraints on the vehicle and cause roughly a 900 lb performance loss. Also, a heads-down attitude after SRB separation is preferred for intact abort considerations. So, two vehicle roll maneuvers are required for what is referred to as a heads-up trajectory in this study. The first roll maneuver occurs after the launch pad is cleared to get the vehicle in a heads-up position; then a second roll maneuver is performed prior to SRB jettison to place the vehicle in a heads-down attitude. Originally, only the single roll maneuver after launch pad clearance was allowed to occur in the MASTRE program. Therefore, an additional roll option needed to be incorporated into the program, and as a result two new inputs were created as follows:

1. HDMACH – Mach number to initiate second roll maneuver.
2. CHRDHD – roll rate for the second roll maneuver in degrees per second.

Note, the second roll maneuver is set up in the program to go from a heads-up attitude to a heads-down attitude only. Otherwise stated, a heads-up attitude to a heads-sideways attitude cannot occur; the vehicle will always roll to heads-down.

Another modification to the program involves the calculation of SSME specific impulse (Isp). The Isp's of the SSMEs is not considered constant but is assumed to vary as a quadratic function of engine rated power level (RPL) as follows:

$$\text{SSME Isp} = C_1 P_L^2 + C_2 P_L + C_3 \quad (2.38)$$

where

C_1, C_2, C_3 – are coefficients of constant value

P_L – engine power level

The previous version of the program required the user to input the coefficients of the above equation. However, the program has been modified to calculate the coefficients based on three input Isp's and their respective power levels. The input variable names are TBLISP and TBLPL for the SSME Isp's and power levels, respectively. This procedure is useful because SSME assessment tag Isp's are given at three different power levels. Overall, this program modification was used to simplify user input.

A final minor modification to the MASTRE program dealt with the input of SRM ballistic performance data (pressure, thrust, flowrate and nozzle throat exit area time histories). The old version of the program required the SRM performance data to be entered in a namelist format (see the Appendix as an example of namelist input). This input method has been changed so the MASTRE program can now read a sequential access file containing the SRM data, and only the name of the file requires input. Therefore, the process of running trajectories using a variety of SRM performance characteristics can easily be accomplished, as required in this study.

E. Trajectory Simulation Groundrules

The groundrules used in an ascent trajectory simulation must be explicitly stated because of the multitude of parameters which can potentially affect the results. However, to include all the groundrules requires a great deal of detail. Therefore, the following is a list of documents and the groundrules they contain, which were necessary for this study.

1. Shuttle Operational Data Submittal (SODS) J-763 Addendum 1 [7] — This document provides all the data required for simulating performance reference mission four (PRM-4). This mission is a baseline trajectory, launched in a polar orbit from the Western Test Range (WTR), and is used for trajectory design. However, not all the inputs for this study were taken from this SODS. The reason for this decision is because some of the data is outdated, and SRM data had to include the effects of various propellant burnrates (R_b 's) as described in item 5. The following information was taken from this SODS:

- a. Launch Site – WTR.
- b. Orbit Destination – 150 nautical miles (n.mi) altitude, inclined 98 deg to the equator.
- c. MECO Targets – Altitude of 57 n.mi., relative velocity (V_R) of 25,374 ft per sec, and relative flight path angle (γ_R) of 0.65 deg.
- d. STS Vehicle Aerodynamics – Integrated Vehicle Baseline Configuration 3 (IVBC-3) aerodynamics.
- e. Launch Site Winds – December mean monthly wind model for WTR.
- f. Launch Site Atmosphere – December Range Reference Atmosphere (RRA) for WTR.
- g. Vehicle Weight Summary Data (except SRM weights).
- h. Propellant Loads – Orbital Maneuvering System (OMS) and Reaction Control System (RCS) loads only.

i. Longitudinal Acceleration – Constrained to a maximum value of 3 G's.

2. Rockwell International Internal Letter, FSD&P/AFS-85-361 [8] — This letter contains information for a heads-down, August launch trajectory, using filament wound case (FWC) SRMs with a burnrate of 0.371 in. per second (ips). Note, all burnrates in this study are referenced to standard conditions of 60°F and 625 psia. Now, accompanying this letter was information for a heads-up, December launch trajectory, using FWC SRMs with 0.392 ips R_b 's. Data for this study was taken from this accompanying heads-up trajectory. Specifically, these data include angle of attack (α) and angle of sideslip (β) Mach number histories, which are consistent with the nominal design requirements established in Reference 7. Also, the vehicle center of gravity (cg) Mach number history was taken from the heads-up trajectory. Note, this cg data incorporates FWC SRMs with R_b 's of 0.392 ips.

3. Main Propulsion System (MPS) Propellant Inventory STS 61-I Revision W [9] — This document contains the propellant loads for the ET. The propellants are liquid oxygen (LOX) and liquid hydrogen (LH₂), and are used by the SSMEs.

4. MSFC Memo EL24 (86-36) [10] — Data contained in this memo are the MPS assessment tags. These data include SSME thrust, flowrate and Isp at various power levels. Note, SSME vacuum thrust at 100 percent RPL is 469,760 lbf.

5. Heads-Up Vandenberg Launch Site (VLS) FWC High Burn Rate SRM Data Submittal [11] and STS-2V(62-B) SRM Data Submittal [12] — These data submittals contain propellant load, mass property, and ballistic performance scaling information for FWC SRMs with R_b 's of 0.368 ips and 0.392 ips, respectively. The information in these data submittals was used to linearly interpolate/extrapolate all the SRM data required in this study. Note that to increase the burnrate of an SRM, iron oxide is added to the propellant. This procedure increases the propellant weight but reduces propellant Isp. Also, because an increased burnrate leads to increased motor chamber pressure, stronger and heavier motor cases are required. Therefore, SRM inert weight also increases with increasing burnrate. The specific linear equations used to account for the above three effects are as follows:

a. Propellant Weight

$$WP = 89208 R_b + 1074388 \quad (2.39)$$

where,

WP – is propellant weight in pound mass (lbm)

R_b – is propellant burnrate in ips.

b. Inert Weight

$$WI = 84542 R_b + 129546 \quad (2.40)$$

where,

WI – is SRM inert weight in lbm.

c. Isp Reduction Multiplier

$$M = - 0.0810583 R_b + 1.0298295 \quad (2.41)$$

where

M – is the ISP reduction multiplier.

Note, that even though the SRM mass properties change with burnrate, the STS vehicle cg Mach number history was assumed constant on all trajectory runs. This assumption was made because the overall vehicle cg is not significantly changed, and so the effect on STS performance is negligible. Again, the cg data for the vehicle was taken from the heads-up trajectory accompanying Reference 8.

The SRM ballistic performance data (time histories of chamber pressure, thrust, flowrate, and nozzle throat exit area) were scaled from an SRM Block II baseline motor designated as TC-MD-271-84-MAX2. This baseline motor had to be scaled to account for burnrate, propellant weight, and propellant mean bulk temperature (PMBT). These empirical scaling equations are as follows:

$$\text{THRUST} = (\text{THB}) (e)^{K_1} (\text{KW})^{1.53846} \quad (2.42)$$

$$\text{PRESSURE} = (\text{PB}) (e)^{K_1} (\text{KW})^{1.53846} \quad (2.43)$$

$$\text{TIME} = (\text{TIB}) (e)^{K_2} (\text{KW})^{-0.53846} \quad (2.44)$$

$$\text{FLOWRATE} = (\text{FLB}) (e)^{K_2} (\text{KW})^{1.53846} \quad (2.45)$$

where THB, PB, TIB, and FLB are thrust, pressure, time, and flowrate of the baseline motor, respectively. Also:

$$K_1 = 0.0011 (\text{PMBTS} - \text{PMBTB}) + 1.567153 \ln (\text{RB}/\text{RBB}) \quad (2.46)$$

$$K_2 = 0.001063 [(\text{PMBTS} - \text{PMBTB}) + 1474.274 \ln (\text{RB}/\text{RBB})] \quad (2.47)$$

$$\text{KW} = \text{WP}/\text{WPB} \quad (2.48)$$

where

PMBTS – PMBT at the launch site in degrees Fahrenheit (depends on launch date)

PMBTB – PMBT of the baseline motor in degrees Fahrenheit

RB – motor burnrate desired in ips

RBB – baseline motor burnrate in ips

WP – propellant weight of motor desired in lbm

WPB – propellant weight of the baseline motor in lbm.

Once a motor was properly scaled, then the Isp reduction multiplier was applied. Also, SRB staging time was set to occur 6.2 sec after the time when chamber pressure, in head end of an SRM, decayed to 50 psia.

6. Roll Maneuver — A roll maneuver of plus or minus 90 deg is required to place the vehicle in a heads-down or heads-up attitude, respectively, along the flight azimuth. The time to initiate the roll maneuver was fixed at 6.4 sec from launch, at a rate of 7.84 deg per second. These values were taken from Reference 8 and are consistent with the roll maneuver to heads-down currently used in STS trajectories. Note, in actuality the vehicle initiates the roll maneuver once a certain velocity is achieved.

7. Roll Maneuver to Heads-Down for an Initially Heads-Up Trajectory — The command to roll the vehicle to heads-down, for an initially heads-up trajectory, was fixed to initiate at a Mach number of 2.5, and a roll rate of 15 degrees per second. The reason for this roll maneuver is explained in the Program Modifications section.

An example of all the namelist input required to run a trajectory using the MASTRE program is displayed in the Appendix. An explanation of all the variables listed is available in Reference 4.

F. Procedure

The procedure used in this study required numerous trajectory runs using the MASTRE program. First, SRM performance and mass property data were generated for sixteen pairs of motors, with propellant burnrates varying from 0.368 ips (current target) to 0.398 ips, at 0.002 ips increments. Note, these SRM data were generated from the information in the Groundrules Section 5, and each pair of SRMs had the same characteristics. Next, SRM data with 0.368 ips burnrate, no maximum Q constraint, and all the trajectory information from the Groundrules section were input into the MASTRE program. Then, the program was executed, and heads-up trajectory was optimized, based on maximizing injection weight, for this case. This process was repeated to attain optimal performance heads-up trajectories, with no max Q constraints, for SRM data with 0.370, 0.372, 0.374, 0.376, 0.378, 0.380, 0.382, 0.384, 0.386, 0.388, 0.390, 0.392, 0.394, 0.396, and 0.398 ips. Next, the entire procedure is repeated implementing max Q constraints of 660, 680, 700, and 720 pounds force per square foot (psf). Therefore, a family of injection weight (payload capability) versus SRM burnrate curves are generated. Finally, for comparison, a heads-down trajectory using a 0.368 ips burnrate SRM and a 680 psf Q constraint was optimized for performance. This case incorporates the current flight conditions.

Note, when maximum Q constraints were implemented, an SSME throttle down was required during first stage flight. For simplicity, the engines were allowed to operate at only 109 percent RPL and 65

percent RPL. Therefore, the time to initiate SSME throttle down to 65 percent RPL, for Q control, was based on satisfying the Q constraint while optimizing performance. Throttle up time (back to 109 percent RPL) occurred six seconds after max Q.

III. RESULTS

The results of this study are summarized in Figure 4, which is a plot of injection weight versus SRM burnrate. This figure shows the heads-up ascent, injection weight achievable for Q constraints of 660 psf, 680 psf, 700 psf, 720 psf, and unconstrained Q; with SRM burnrates ranging from 0.368 ips to 0.398 ips by 0.002 ips increments. The heads-down ascent (current flight mode), injection weight of 318,217 lbm, for an SRM burnrate of 0.368 ips, is shown for comparison. The unconstrained Q curve is essentially linear, with injection weight increasing with increasing SRM burnrate. The maximum injection weight value on this curve is 326,064 lbm, which occurs at an SRM burnrate of 0.398 ips and Q of 823 psf. For Q constrained to 660 psf, the curve is nonlinear with injection weight increasing with SRM burnrate, to a maximum value of 321,556 lbm at 0.390 ips. Thereafter, injection weight decreases with increasing SRM burnrate. The curve with a Q constraint of 680 psf is nonlinear, and injection weight increases with increasing SRM burnrate to a maximum value of 322,510 lbm, at 0.394 ips. Injection weight decreases with increasing SRM burnrate thereafter. The curves with Q constraints of 700 and 720 psf are also nonlinear. Both of these curves display injection weight increasing with increasing SRM burnrate, with respective maximum values of 323,416 lbm and 324,103 lbm both occurring at 0.398 ips.

Tables 1, 2, 3, 4, and 5 contain the injection weight and SRM burnrate values used to generate Figure 4. Table 1 displays this information for unconstrained Q; whereas, Tables 2 through 5 display these data for Q constraints of 660 psf, 680 psf, 700 psf, and 720 psf, respectively. Tables 1 through 5 also list the following parameters: ignition weight, delta injection weight (heads-up value minus the baseline heads-down value), minimum product of dynamic pressure and angle of attack ($Q\alpha$), minimum $Q\alpha$ time, max Q, max Q time, MECO time, and initiation of throttle down to 65 percent RPL time. Recall that the MECO and throttle down times are control parameters in the optimization scheme.

The remainder of the results are mission elapsed time (MET) history plots of a variety of parameters and an altitude versus range plot. These figures compare the baseline heads-down ascent trajectory to the heads-up ascent trajectory with Q constrained to 680 psf and an SRM R_b of 0.394 ips. This particular heads-up case was chosen for comparison to the baseline because 680 psf is a mission nominal design Q, and an SRM burnrate of 0.394 ips provided the optimum (maximum) injection weight at this Q. A discussion of each figure follows:

Figure 5 — Compares the vacuum thrust-time traces for individual SRMs with burnrates of 0.368 ips (used in the baseline heads-down trajectory) and 0.394 ips (used in the heads-up trajectory). The 0.394 ips motor provides significantly more impulse prior to 80 sec than the 0.368 ips burnrate motor. In particular, the total impulses at 60 sec are 170.034×10^6 lbf-sec and 186.500×10^6 lbf-sec for the 0.368 ips and 0.394 ips motors, respectively. The difference between these values is 16.466×10^6 lbf-sec. However, at action time (motor burnout) the total impulses are 293.715×10^6 lbf-sec and 293.732×10^6 lbf-sec for the 0.368 ips and 0.394 ips burnrates SRMs, respectively. These values differ by only 0.017×10^6 lbf-sec.

Figure 6 — Shows SSME power level time histories during first stage, for the heads-up and heads-down trajectories. The second stage power level time history is constant at 109 percent RPL until initiation

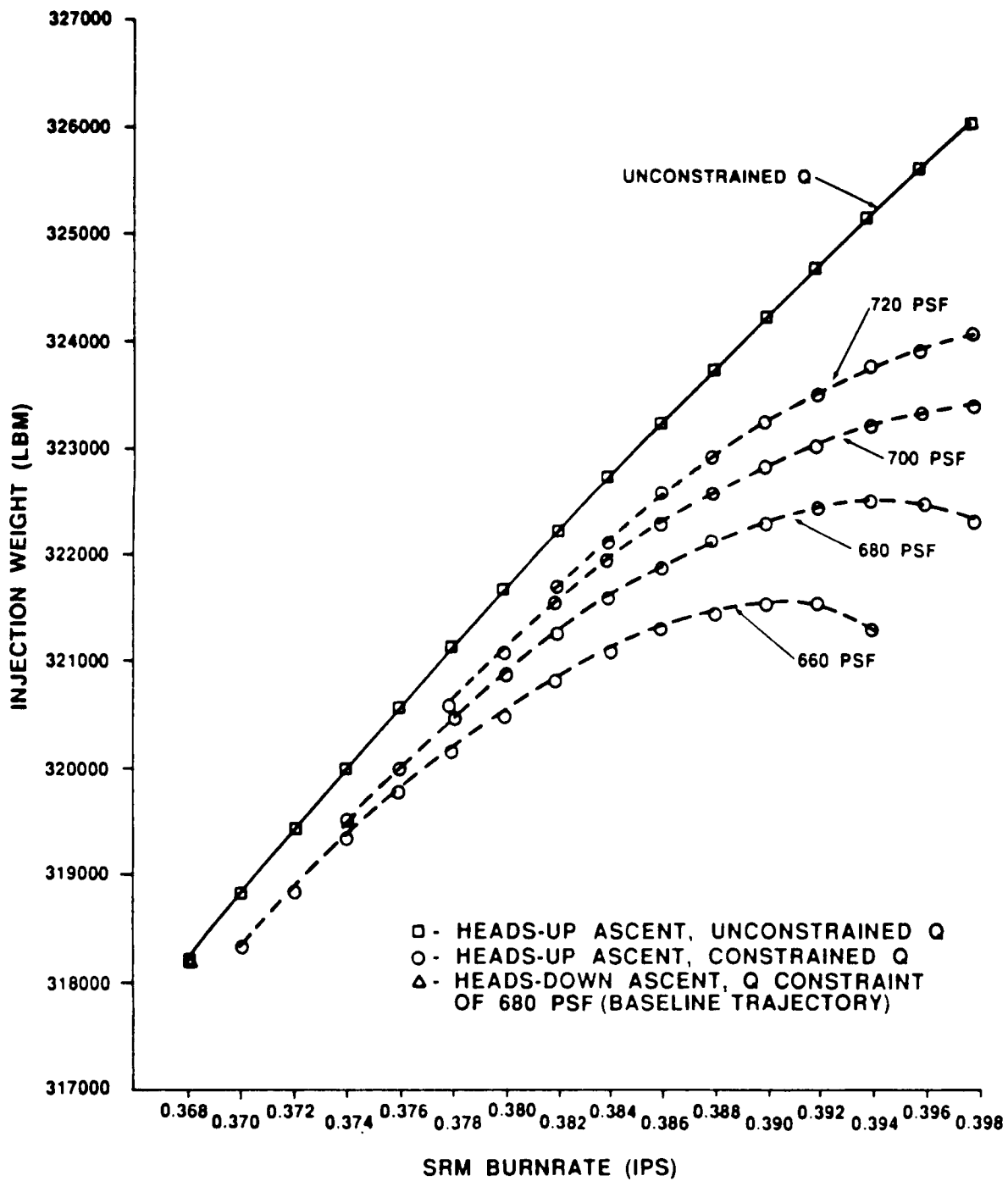


Figure 4. Heads-up injection weight comparison.

TABLE 1. HEADS-UP PERFORMANCE/TRAJECTORY SUMMARY FOR UNCONSTRAINED Q

CASE	SRM R _b (ips)	IGNITION WEIGHT (lbm)	INJECTION WEIGHT (lbm)	DELTA INJECTION WEIGHT† (lbm)	Q α MIN (psf x degrees)	Q α MIN TIME (sec)	Q MAX (psf)	Q MAX TIME (sec)	MECO TIME (sec)	65% THROTTLE DOWN TIME (sec)
B *	0.368	4450863	318217	-	-3049	50.75	680	52.04	496.42	28.36
1	0.368	4450863	318224	7	-2960	52.25	662	51.73	485.34	‡
2	0.370	4451557	318828	611	-3006	51.84	672	51.33	485.06	‡
3	0.372	4452253	319442	1225	-3053	51.50	682	50.96	484.79	‡
4	0.374	4452947	320002	1785	-3100	51.00	693	50.61	484.53	‡
5	0.376	4453643	320573	2356	-3148	50.76	703	50.26	484.27	‡
6	0.378	4454337	321132	2915	-3196	50.50	714	49.93	484.02	‡
7	0.380	4455035	321672	3455	-3244	50.00	724	49.61	483.77	‡
8	0.382	4455729	322207	3990	-3292	49.29	735	49.29	483.53	‡
9	0.384	4456423	322728	4511	-3340	48.75	746	48.98	483.29	‡
10	0.386	4457119	323238	5021	-3388	48.25	756	48.68	483.07	‡
11	0.388	4457813	323733	5516	-3436	47.75	767	48.39	482.84	‡
12	0.390	4458509	324217	6000	-3483	47.25	778	48.12	482.62	‡
13	0.392	4459191	324694	6477	-3531	47.00	789	47.75	482.41	‡
14	0.394	4459897	325162	6945	-3579	46.50	800	47.59	482.20	‡
15	0.396	4460593	325617	7400	-3628	46.25	811	47.35	482.00	‡
16	0.398	4461287	326064	7847	-3676	46.00	823	47.12	481.80	‡

* BASELINE: HEADS-DOWN

† RELATIVE TO BASELINE

‡ NO THROTTLE DOWN REQUIRED FOR UNCONSTRAINED Q

TABLE 2. HEADS-UP PERFORMANCE/TRAJECTORY SUMMARY, Q CONSTRAINT OF 660 PSF

CASE	SRM R _b (ips)	IGNITION WEIGHT (lbm)	INJECTION WEIGHT † (lbm)	DELTA INJECTION WEIGHT (lbm)	Q α MIN (psf x degrees)	Q α MIN TIME (sec)	Q MAX (psf)	Q MAX TIME (sec)	MECO TIME (sec)	65% THROTTLE DOWN TIME (sec)
B *	0.368	4450863	318217	-	-3049	50.75	680	52.04	496.42	28.36
2	0.370	4451557	318308	91	-2971	47.00	660	47.44	487.81	45.17
3	0.372	4452253	318827	610	-2976	45.93	660	45.68	487.98	42.38
4	0.374	4452947	319347	1130	-2970	45.75	660	44.33	488.07	40.22
5	0.376	4453643	319797	1580	-2973	46.25	660	43.98	488.47	38.36
6	0.378	4454337	320170	1953	-2975	45.00	660	44.29	489.21	36.40
7	0.380	4455035	320515	2298	-2976	44.75	660	44.57	490.01	34.29
8	0.382	4455729	320836	2619	-2976	44.50	660	44.75	490.87	32.04
9	0.384	4456423	321116	2899	-2975	44.25	660	45.15	491.84	29.61
10	0.386	4457119	321337	3120	-2972	44.25	660	45.58	492.96	27.00
11	0.388	4457813	321453	3236	-2970	44.25	660	45.98	494.22	24.11
12	0.390	4458509	321550	3333	-2966	44.75	660	46.25	495.55	20.95
13	0.392	4459191	321556	3339	-2965	45.00	660	46.50	497.04	17.03
14 ‡	0.394	4459897	321297	3080	-2964	45.50	660	46.79	499.05	14.77

* BASELINE: HEADS-DOWN

† RELATIVE TO BASELINE

‡ THROTTLE LEVEL 100% RP1 BEFORE BUCKET, 109% AFTER BUCKET

TABLE 3. HEADS-UP PERFORMANCE/TRAJECTORY SUMMARY, Q CONSTRAINT OF 680 PSF

CASE	SRM R _b (ips)	IGNITION WEIGHT (lbm)	INJECTION WEIGHT (lbm)	DELTA INJECTION WEIGHT † (lbm)	Q α MIN (psf x degrees)	Q α MIN TIME (sec)	Q MAX (psf)	Q MAX TIME (sec)	MECO TIME (sec)	65% THROTTLE DOWN TIME (sec)
B*	0.368	4450863	318217	-	-3049	50.75	680	52.04	496.42	28.36
4	0.374	4452947	319484	1267	-3058	46.25	680	46.76	487.31	44.39
5	0.376	4453643	319983	1766	-3065	44.75	680	45.00	487.47	41.69
6	0.378	4454337	320479	2262	-3066	44.25	680	43.75	487.58	39.57
7	0.380	4455035	320893	2676	-3066	44.00	680	43.50	488.03	37.75
8	0.382	4455729	321248	3031	-3066	43.75	680	43.80	488.77	35.79
9	0.384	4456423	321570	3353	-3065	43.50	680	44.10	489.58	33.70
10	0.386	4457119	321865	3648	-3063	43.25	680	44.45	490.49	31.44
11	0.388	4457813	322117	3900	-3061	43.25	680	44.75	491.46	29.03
12	0.390	4458509	322269	4052	-3058	43.50	680	45.20	492.63	26.38
13	0.392	4459191	322421	4204	-3055	43.75	680	45.49	493.83	23.51
14	0.394	4459897	322510	4293	-3052	44.25	680	45.75	495.16	20.33
15	0.396	4460593	322491	4274	-3050	44.50	680	45.93	496.64	16.34
16	0.398	4461287	322295	4078	-3050	44.75	680	46.01	498.22	11.11

* BASELINE: HEADS-DOWN

† RELATIVE TO BASELINE

TABLE 4. HEADS-UP PERFORMANCE/TRAJECTORY SUMMARY, Q CONSTRAINT OF 700 PSF

CASE	SRM R_b (ips)	IGNITION WEIGHT (lbm)	INJECTION WEIGHT (lbm)	DELTA INJECTION WEIGHT† (lbm)	Q α MIN (psf x degrees)	Q α MIN TIME (sec)	Q MAX (psf)	Q MAX TIME (sec)	MECO TIME (sec)	65% THROTTLE DOWN TIME (sec)
B*	0.368	4450863	318217	—	-3049	50.75	680	52.04	496.42	28.36
6	0.378	4454337	320609	2392	-3144	45.50	700	46.07	486.85	43.59
7	0.380	4455035	321082	2865	-3152	43.75	700	44.43	487.02	40.99
8	0.382	4455729	321560	3343	-3156	43.00	700	43.15	487.12	38.93
9	0.384	4456423	321943	3726	-3156	42.75	700	43.07	487.62	37.13
10	0.386	4457119	322269	4052	-3155	42.50	700	43.42	488.40	35.19
11	0.388	4457813	322564	4347	-3152	42.25	700	43.76	489.24	33.09
12	0.390	4458509	322841	4624	-3149	42.50	700	44.00	490.13	30.82
13	0.392	4459191	323026	4809	-3146	42.75	700	44.42	491.17	28.40
14	0.396	4459897	323210	4993	-3142	43.00	700	44.77	492.30	25.73
15	0.394	4460593	323342	5125	-3139	43.50	700	45.00	493.50	22.82
16	0.398	4461287	323416	5199	-3137	43.75	700	45.20	494.79	19.67

* BASELINE: HEADS-DOWN

† RELATIVE TO BASELINE

TABLE 5. HEADS-UP PERFORMANCE/TRAJECTORY SUMMARY, Q CONSTRAINT OF 720 PSF

CASE	SRM R _b (ips)	IGNITION WEIGHT (lbm)	INJECTION WEIGHT † (lbm)	DELTA INJECTION WEIGHT (lbm)	Q α MIN (psf x degrees)	Q α MIN TIME (sec)	Q MAX TIME (psf)	Q MAX TIME (sec)	MECO TIME (sec)	65% THROTTLE DOWN TIME (sec)
B*	0.368	4450863	318217	—	-3049	50.75	680	52.04	496.42	28.36
8	0.382	4455729	321683	3466	-3230	44.75	720	45.36	486.41	42.75
9	0.384	4456423	322134	3917	-3238	43.25	720	43.84	486.59	40.27
10	0.386	4457119	322590	4373	-3243	42.00	720	42.61	486.69	38.27
11	0.388	4457813	322928	4711	-3244	41.50	720	42.75	487.32	36.49
12	0.390	4458509	323230	5013	-3241	41.50	720	43.13	488.10	34.54
13	0.392	4459191	323511	5294	-3237	41.75	720	43.44	488.95	32.43
14	0.394	4459897	323771	5554	-3233	42.00	720	43.70	489.80	30.19
15	0.396	4460593	323933	5716	-3230	42.50	720	44.06	490.89	27.72
16	0.398	4461287	324103	5886	-3227	42.75	720	44.32	491.99	25.05

* BASELINE: HEADS-DOWN

† RELATIVE TO BASELINE

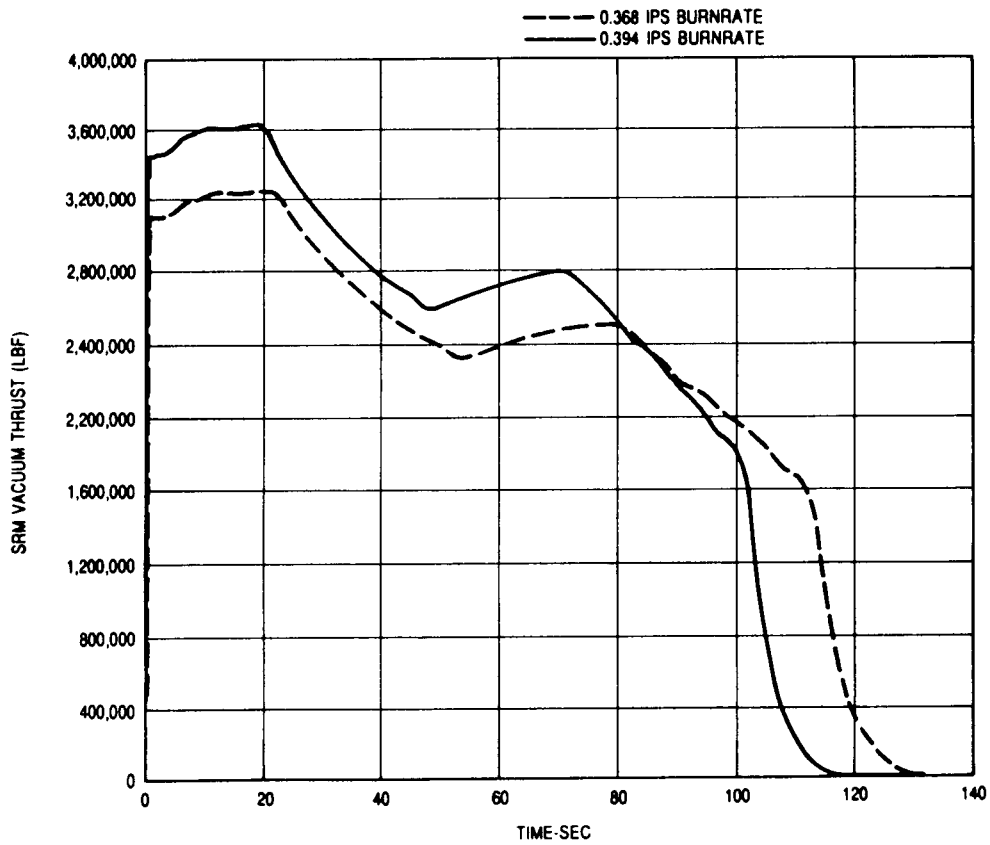


Figure 5. SRM vacuum thrust comparison.

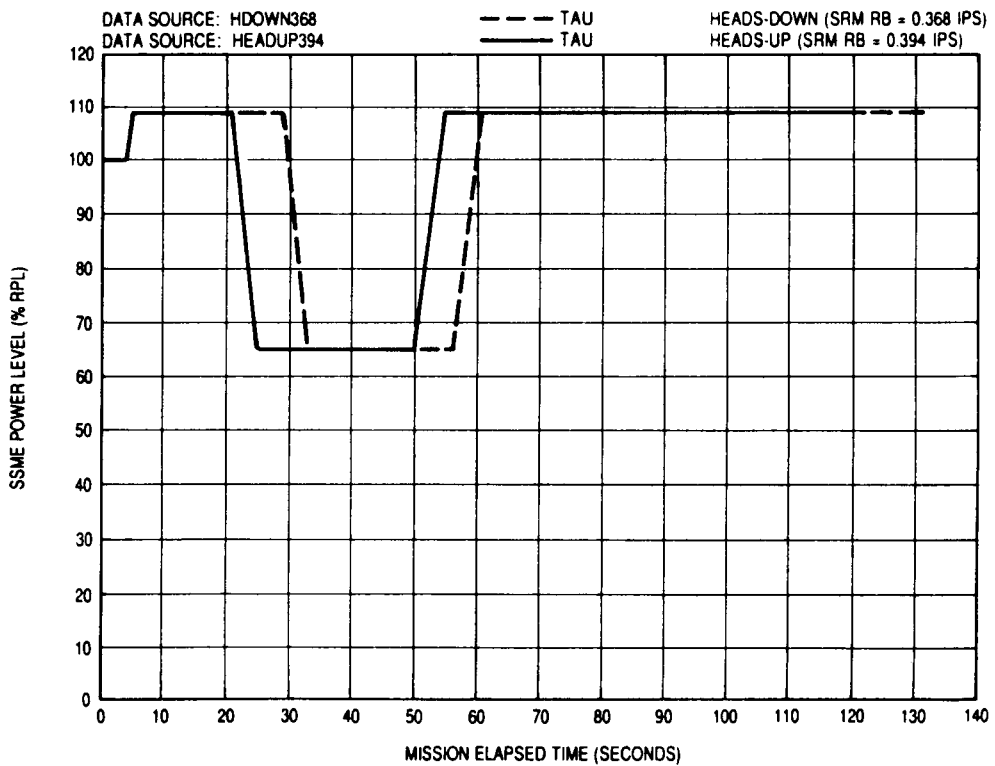


Figure 6. Heads-up versus heads-down SSME power level comparison.

of 3-G throttling. Recall, 100 percent RPL is roughly equivalent to a vacuum thrust of 469,760 lbf. The initiation of Q control throttle down to 65 percent occurs at 28.36 sec for the heads-down case, and at 20.33 sec for the heads-up case. These times are optimized values, since the throttle down time is a control parameter in this study. Also, these throttle down times are consistent with the fact that the heads-up SRM provides more impulse early in flight, compared to the heads-down motor.

Figure 7 — Is an altitude versus MET plot of the heads-down and heads-up trajectories. Of particular interest is that the heads-up ascent flies a lofted profile relative to the heads-down ascent, until roughly 300 sec. After 300 sec the altitude profiles are essentially the same, because both trajectories have the same MECO altitude target (or terminal constraint).

Figure 8 — Plots range versus MET for the heads-down and heads-up trajectories. Both range time histories have similar signatures. However, the heads-up ascent maintains a further down-range distance, relative to the heads-down ascent, from 100 sec to MECO.

Figure 9 — Shows the altitude versus range flight profile of the heads-down and heads-up trajectories, thus combining Figures 6 and 7. Like Figure 6, examination of this plot shows the heads-up ascent flies a lofted profile relative to the heads-down ascent.

Figure 10 — Displays the relative velocity (V_R) time histories of the heads-down and heads-up ascents. These relative velocity profiles are similar from SRB ignition to 50 sec, with the heads-up ascent velocity profile being consistently faster than the heads-down velocity profile. However, from 50 sec to approximately 120 sec, a significant difference exists between the velocity profiles. This difference is roughly 250 m/sec at 100 sec. The velocity profiles are again similar from roughly 120 sec to MECO; although, the heads-up trajectory maintains a higher velocity throughout this time period than the heads-down trajectory. However, the same target velocity is achieved at MECO in both cases.

Figure 11 — Is a plot of relative flight path angle (γ_R) versus MET of the heads-down and heads-up trajectories. This angle is measured in the pitch plane from the ET centerline to the local horizontal. Examination of the plot reveals that the heads-up ascent has larger values for γ_R until approximately 60 sec, relative to the heads-down ascent. From 60 sec to roughly 125 sec the heads-down ascent γ_R is greater than the heads-up ascent. Finally, from 125 sec to MECO the γ_R profiles are essentially the same because both trajectories must hit the same MECO target. Also, this plot is consistent with the heads-up ascent flying a more lofted trajectory than the heads-down ascent.

Figure 12 — Shows the angle of attack (α) time histories of the heads-down and heads-up trajectories. This angle is measured in the pitch plane, from the ET centerline to the projection of the relative velocity vector. During first stage, after vertical rise and roll to flight azimuth maneuvers, these time histories should have the same signatures. The reason for this condition is due to the fact that in both trajectories, the same α -Mach number history is flown during the first stage pitchover (tilt) sequence. Examination of the plot shows that the signatures are indeed the same from roughly 25 sec to 130 sec. From 150 sec to 450 sec, the heads-up ascent flies a more negative α than the heads-down ascent. Then from 450 sec to MECO, the heads-up ascent α is greater than that of the heads-down ascent. Note, the discontinuities in the α profile (where α jumps to zero degrees), between 100 and 130 sec, is due to an input problem. The α -Mach number history input table did not contain enough values required to get the vehicle to the staging time. Therefore, the MASTRE program assumed an α of zero once the input table ran out. However, all the α -Mach number history data available in Reference 8 was used in the input table. The problem would have

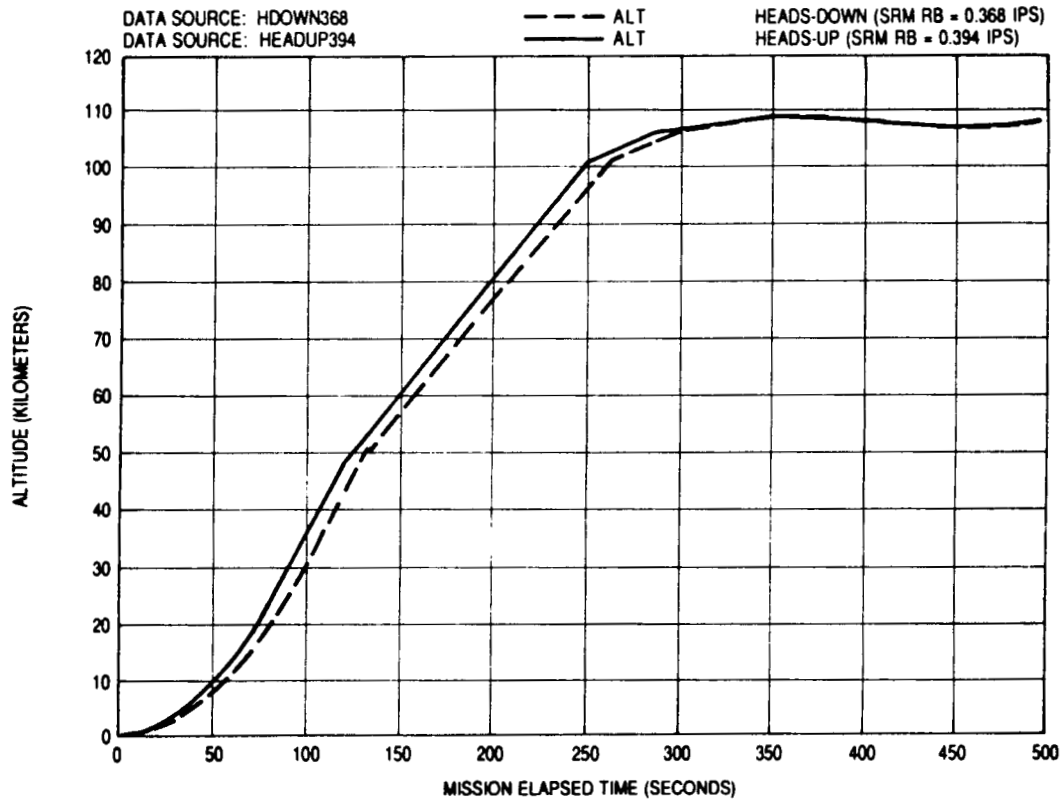


Figure 7. Heads-up versus heads-down altitude comparison.

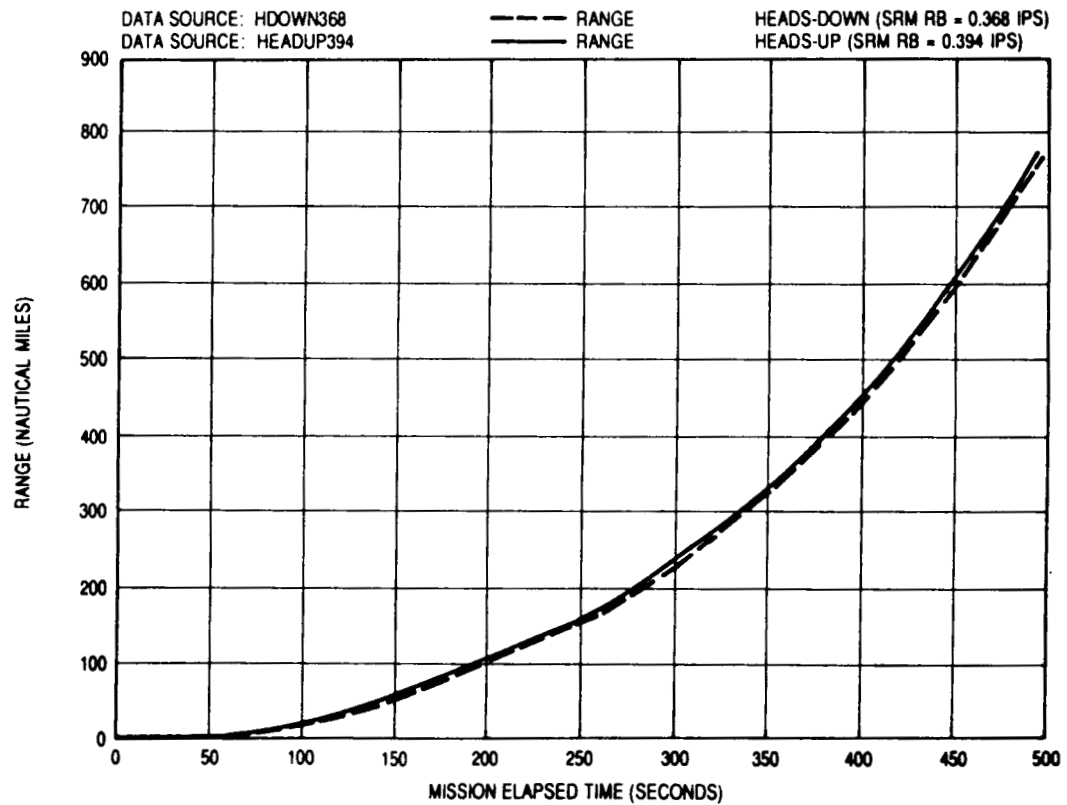


Figure 8. Heads-up versus heads-down range comparison.

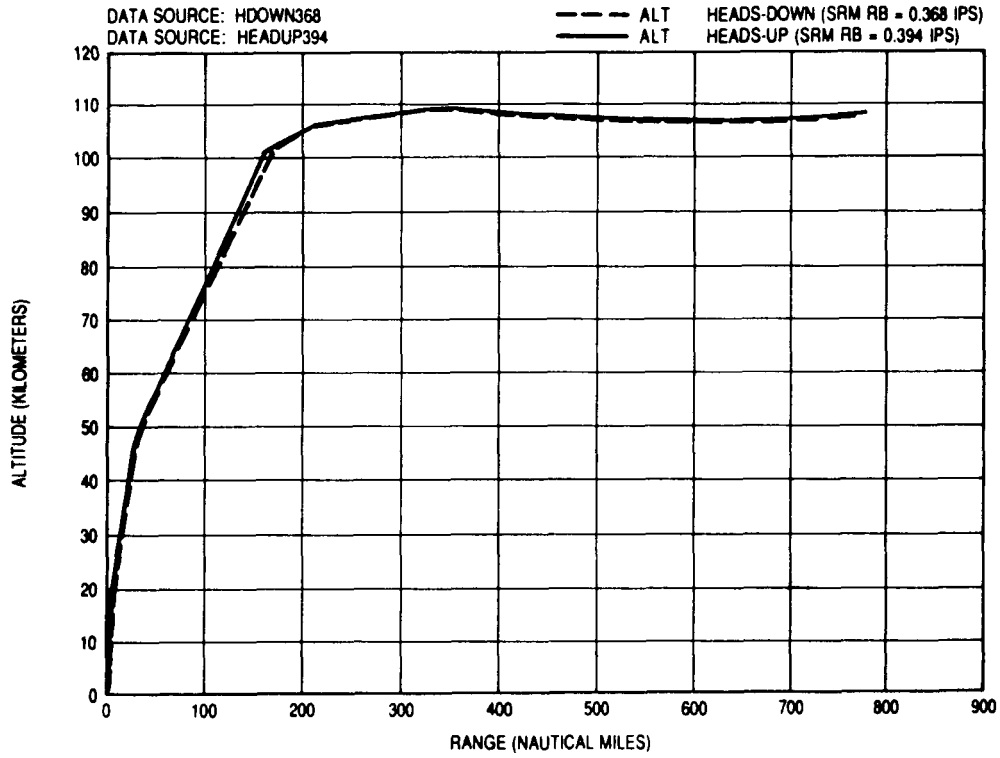


Figure 9. Heads-up versus heads-down altitude/range comparison.

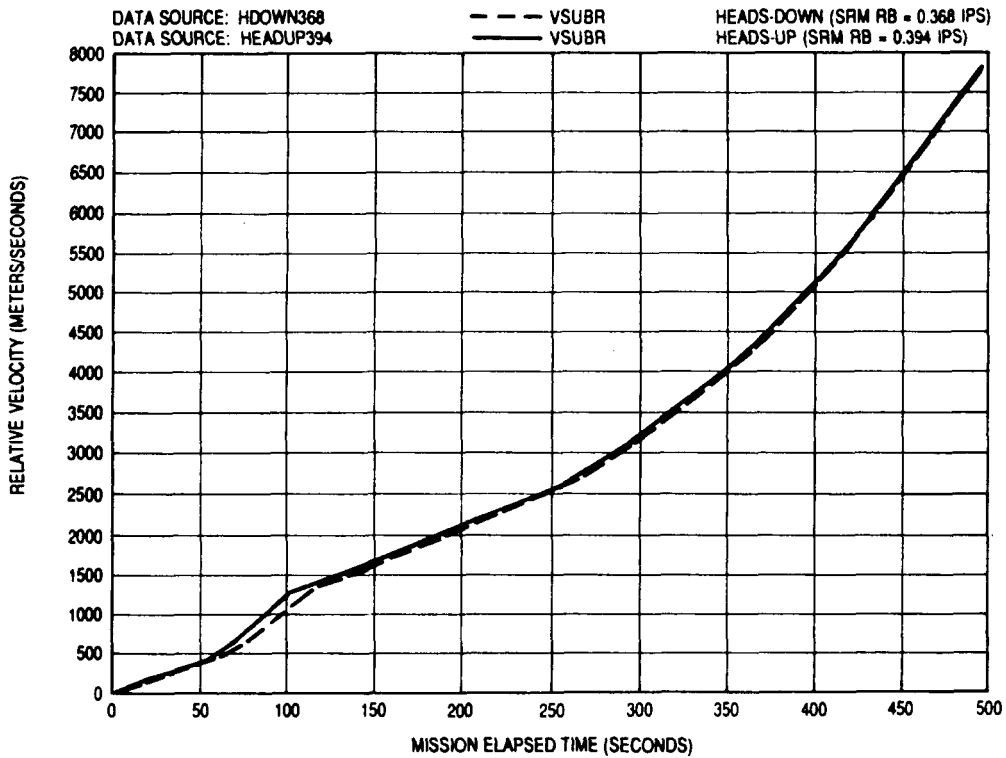


Figure 10. Heads-up versus heads-down relative velocity comparison.

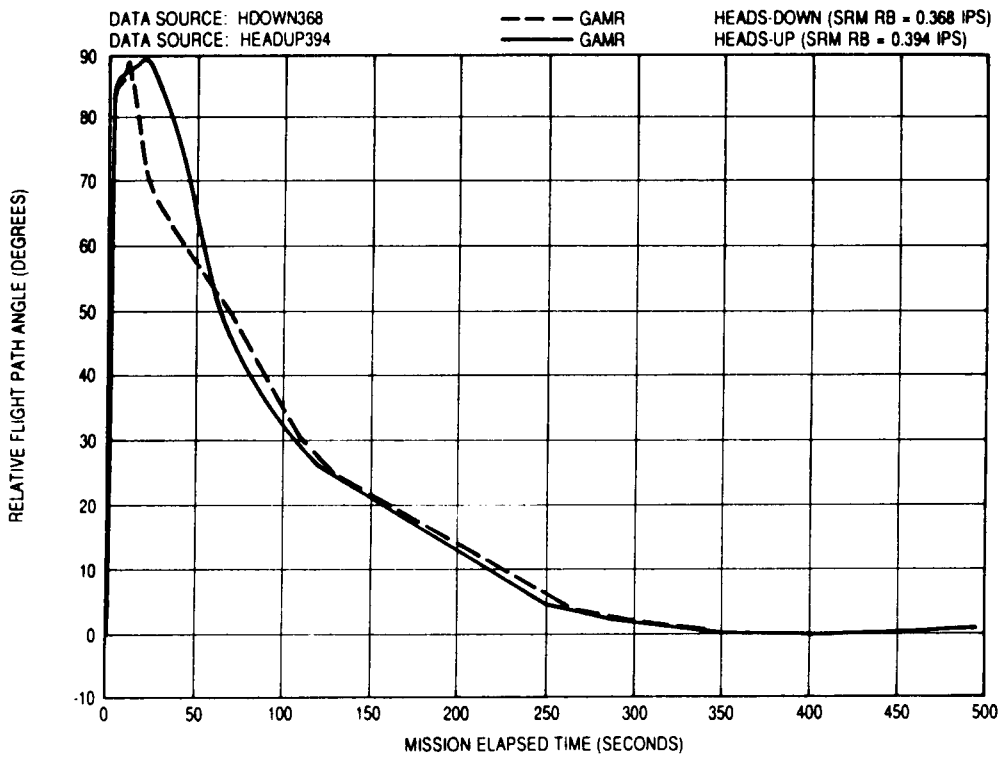


Figure 11. Heads-up versus heads-down relative gamma comparison.

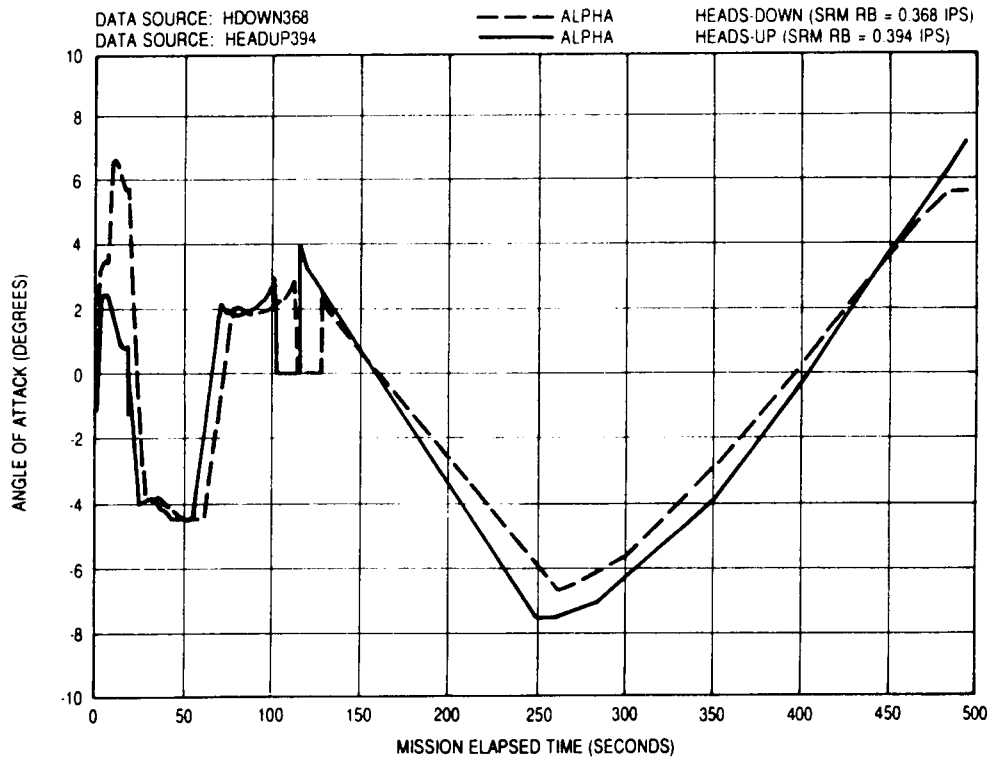


Figure 12. Heads-up versus heads-down alpha comparison.

been alleviated by adding additional Mach number values to the table, which holds the last α value in Reference 8. Obviously, these discontinuities will be observed in the $Q\alpha$ time history, and will also manifest in the χ_P time history to a lesser degree. Since this input problem is of short duration and does not effect the min-H attitude control phase of the program, no significant difference would be observed in the optimized injection weight. Therefore, no updated trajectories were generated.

Figure 13 — Displays the angle of sideslip (β) versus MET for the heads-down and heads-up trajectories. Note, β is measured from the ET centerline to the projection of the relative velocity vector, in the yaw plane. The two β profiles, like the α profiles, have the same signatures during the pitchover phase from roughly 25 sec to 130 sec. This condition results because the same β -Mach number history is flown during first stage pitchover sequence. The second stage profiles, from approximately 130 to MECO, are also similar. However, the heads-up ascent maintains greater values of β relative to the heads-down ascent, during this time period. Note, discontinuities (where β jumps to a value of zero) exist in the β time histories. This situation, like the α time history discontinuities, is due to the lack of sufficient data being supplied in the input β -Mach number history table. These discontinuities will obviously be present in the $Q\beta$ time history and will also manifest itself, to a smaller degree, in χ_Y . Again, since this problem is of short duration and prior to the min-H attitude control phase, no significant difference would be observed in the optimized injection weight. Therefore, no updated trajectories were generated.

Figure 14 — Shows the Mach number time histories of the heads-down and heads-up trajectories. The Mach number profiles have similar signatures as their respective V_R profiles, as expected. The Mach number histories are similar from SRB ignition to 50 sec, with the heads-up ascent having consistently higher Mach number values relative to the heads-down ascent. However, significant differences exist between the two profiles from 50 sec to roughly 120 sec. This difference is about 0.50 at 100 sec. The Mach number profiles are again similar from approximately 120 sec to MECO; with the heads-up trajectory maintaining higher Mach number values relative to the heads-down trajectory during this time frame.

Figure 15 — Is a plot of pitch attitude angle (χ_P) versus MET for the heads-down and heads-up trajectories. The heads-up trajectory has substantially smaller values of χ_P , relative to the heads-down trajectory, from SRB ignition to roughly 50 sec. This situation is consistent with lofted trajectory of the heads-up ascent relative to the heads-down ascent. From 50 sec to roughly 125 sec, the heads-up ascent has larger χ_P values than the heads-down ascent. After 125 sec, both χ_P time histories are essentially the same. Recall, χ_P is a control parameter in the MASTRE program and therefore, these profiles are optimized to maximize vehicle injection weight.

Figure 16 — Shows the yaw attitude angle (χ_Y) time histories for the heads-down and heads-up ascents. The χ_Y profiles are significantly different from SRB ignition until about 20 sec, due to one profile rolling to heads-down while the other rolls to heads-up. Note that roll and yaw are coupled. The profiles are basically similar from 20 sec to approximately 125 sec, with the heads-up ascent having consistently larger values of χ_Y compared to the heads-down ascent. However, at roughly 80 sec, the heads-up χ_Y time history has a local peak which does not appear in heads-down ascent. This peak occurs because during this time frame the vehicle achieves a Mach number of 2.5 and thus triggers the heads-up ascent to roll to heads-down. The reason for the roll to heads-down, for an initially heads-up trajectory, is given in the Program Modifications section. Finally, from roughly 125 sec to MECO, the χ_Y values for both cases are essentially the same. Also, recall χ_Y is optimized by the MASTRE program to maximize vehicle injection weight, since it is a control parameter.

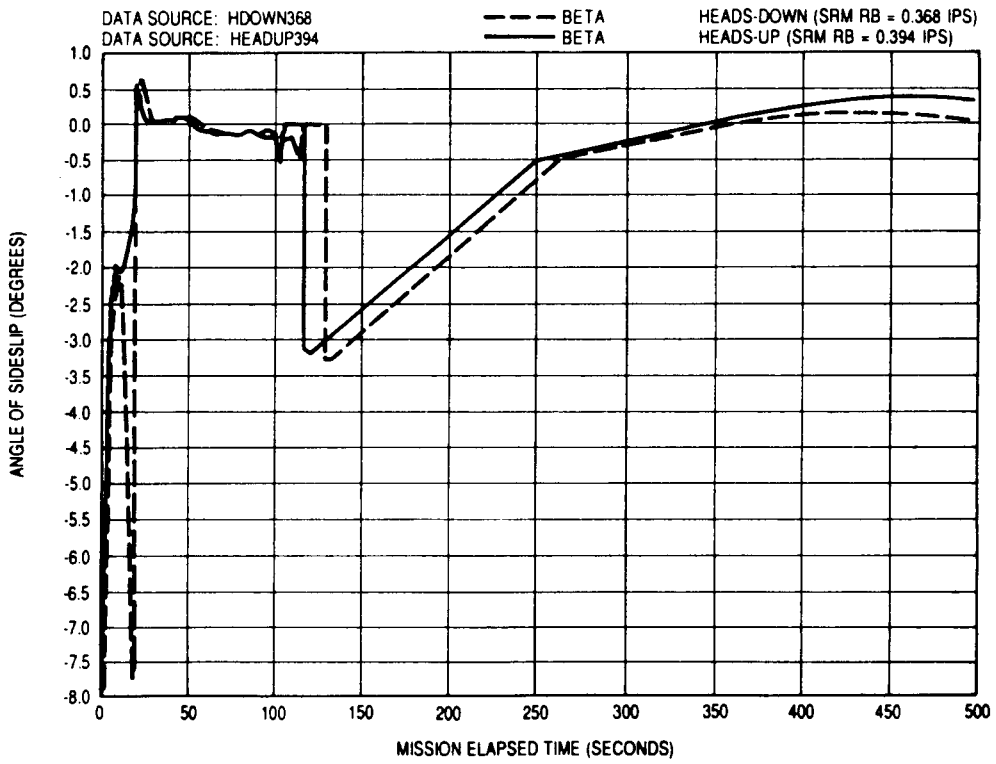


Figure 13. Heads-up versus heads-down beta comparison.

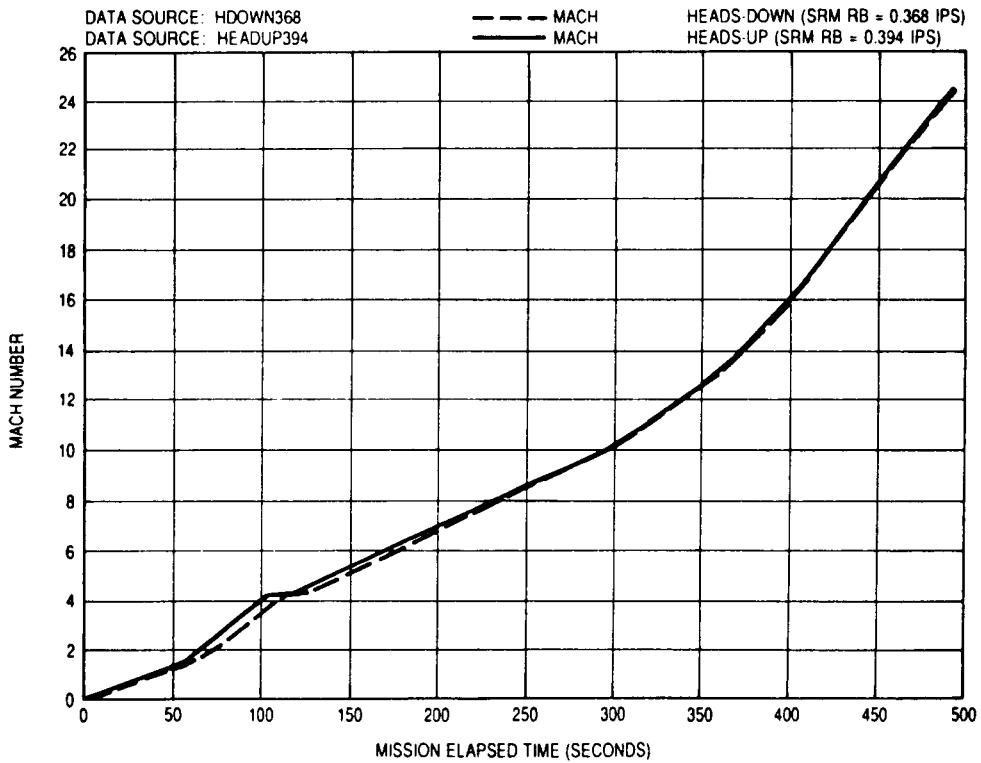


Figure 14. Heads-up versus heads-down Mach number comparison.

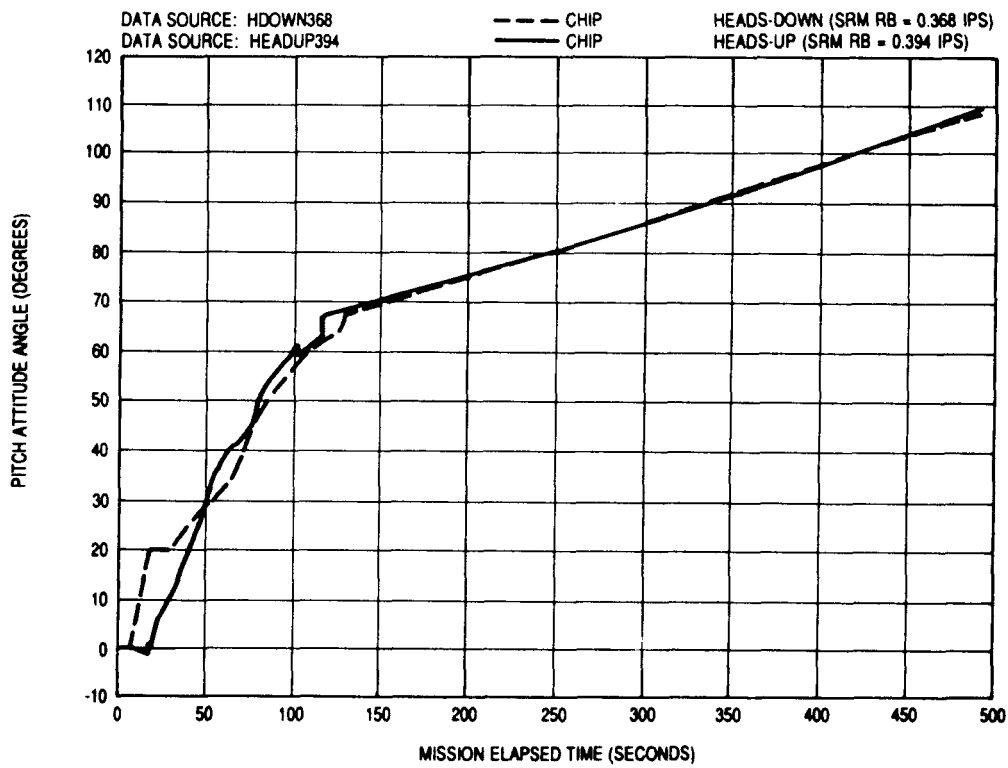


Figure 15. Heads-up versus heads-down chi-pitch comparison.

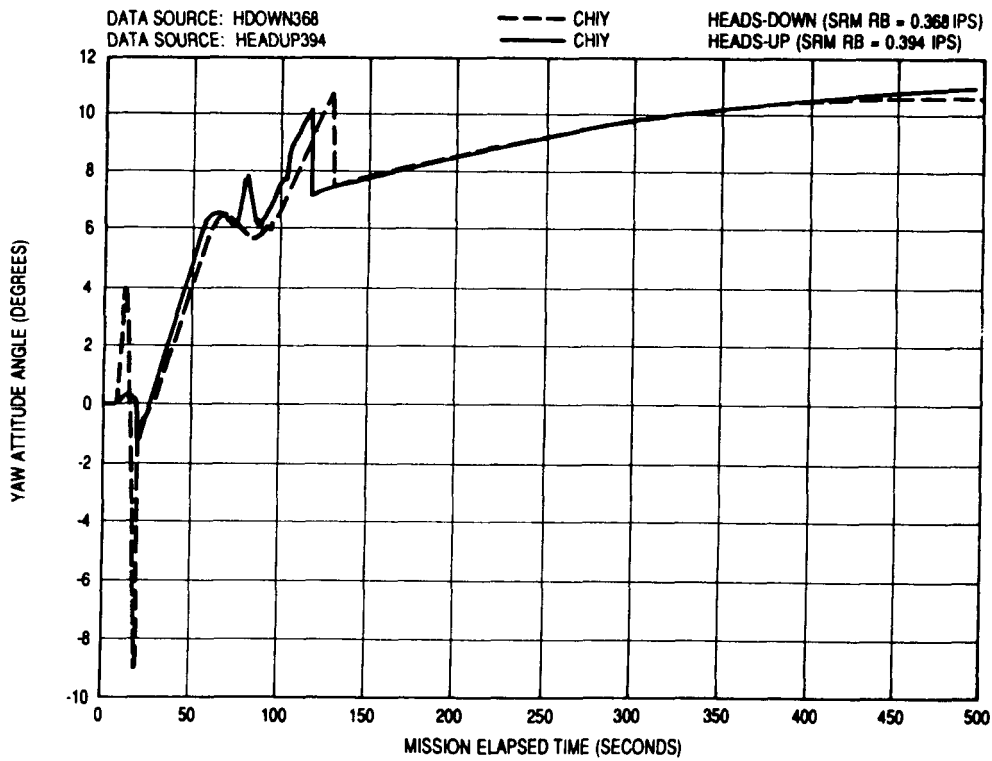


Figure 16. Heads-up versus heads-down chi-yaw comparison.

Figure 17 — Displays the roll attitude angle (χ_R) time histories for the heads-down and heads-up trajectories. The roll maneuvers, after launch pad clearance, can readily be observed in the plot from 6.4 sec to roughly 18 sec for both ascent profiles. The heads-down ascent rolls from χ_R of 90 deg to 180 deg; whereas, the heads-up ascent rolls from 90 deg to 0 deg. Also, for the heads-up ascent, the roll maneuver to heads-down can be seen in the plot from roughly 80 sec to 92 sec, where χ_R ramps from 0 deg to 180 deg. Recall, this second roll maneuver increases performance for reasons stated in the Program Modifications section, and is triggered to initiate when the vehicle attains a Mach number of 2.5. Note, the discontinuities in the plot, where the value of χ_R jumps from 180 deg to -180 deg (or vice-versa), are misleading. A χ_R value of 180 deg or -180 deg, after the roll maneuver to flight azimuth, are actually the same attitude position.

Figure 18 — Is a plot of dynamic pressure (Q) versus MET for the heads-down and heads-up ascents. Only the first stage time history of Q is shown because Q is essentially zero during second stage. Both ascent cases have the typical bell shaped Q profile, and they were both constrained to the same maximum value of 680 psf. However, max Q occurs at 45.75 sec for the heads-up trajectory and at 52.04 sec for the heads-down trajectory. Therefore, a difference of 6.29 sec is observed in the max Q time values between the two cases.

Figure 19 — Shows the product of dynamic pressure with angle of attack ($Q\alpha$) time histories for the heads-down and heads-up trajectories. Only the first stage $Q\alpha$ time histories are shown because $Q\alpha$ is essentially zero during second stage. The signatures of these $Q\alpha$ profiles are the same because both ascent cases are required to fly the same α profile during the tiltover sequence. Note, α tiltover control initiates at 18.4 sec and continues through staging; whereas, initial tiltover from 6.4 sec to 18.3 sec, is optimized by the MASTRE program. Also, the minimum $Q\alpha$ values of -3049 psf-deg and -3052 psf-deg for the heads-down and heads-up ascents, respectively, are approximately the same. However, the heads-up ascent minimum $Q\alpha$ occurs 6.5 sec earlier than that of the heads-down ascent. These minimum $Q\alpha$ values are consistent with the PRM-4 design $Q\alpha$ of -3000 psf-deg, as stated in Reference 7. The discontinuities in the $Q\alpha$ time histories (where $Q\alpha$ jumps to a value of zero psf-deg), between 100 and 130 sec, is due to the input α -Mach number history table not being of sufficient length.

Figure 20 — Displays the product of dynamic pressure with angle of sideslip ($Q\beta$) versus MET for the heads-down and heads-up trajectories. Only the first stage values of $Q\beta$ are shown because $Q\beta$ is essentially zero during second stage. Both trajectories have similar $Q\beta$ profiles during the tiltover sequence, from 18.3 sec to staging, because the same β -Mach number history is input. However, during the initial roll maneuvers, from 6.4 sec to approximately 18 sec, large differences exist in the $Q\beta$ profiles. The heads-down ascent achieves a minimum $Q\beta$ value of roughly -1250 psf-deg; whereas, the heads-up only drops to a minimum of approximately -250 psf-deg. This difference occurs because one trajectory case rolls to heads-down and the other rolls to heads-up, and yaw and roll are coupled. The discontinuities in the $Q\beta$ profiles (where $Q\beta$ jumps to 0 psf-deg), between 100 and 130 sec, is due to insufficient length of the input β -Mach number history table.

Figure 21 — Is a plot of axial (longitudinal) acceleration versus MET for the heads-down and heads-up ascents. The acceleration profiles during second stage, from roughly 125 sec to MECO, are almost identical. Note, the maximum vehicle acceleration was constrained to 3 G's in both cases. However, the first stage time histories are significantly different, with the heads-up ascent having higher values of acceleration than those of the heads-down ascent. This condition is a direct result of higher thrust provided by the 0.394 ips burnrate SRM relative to the 0.368 ips burnrate SRM (Fig. 5).

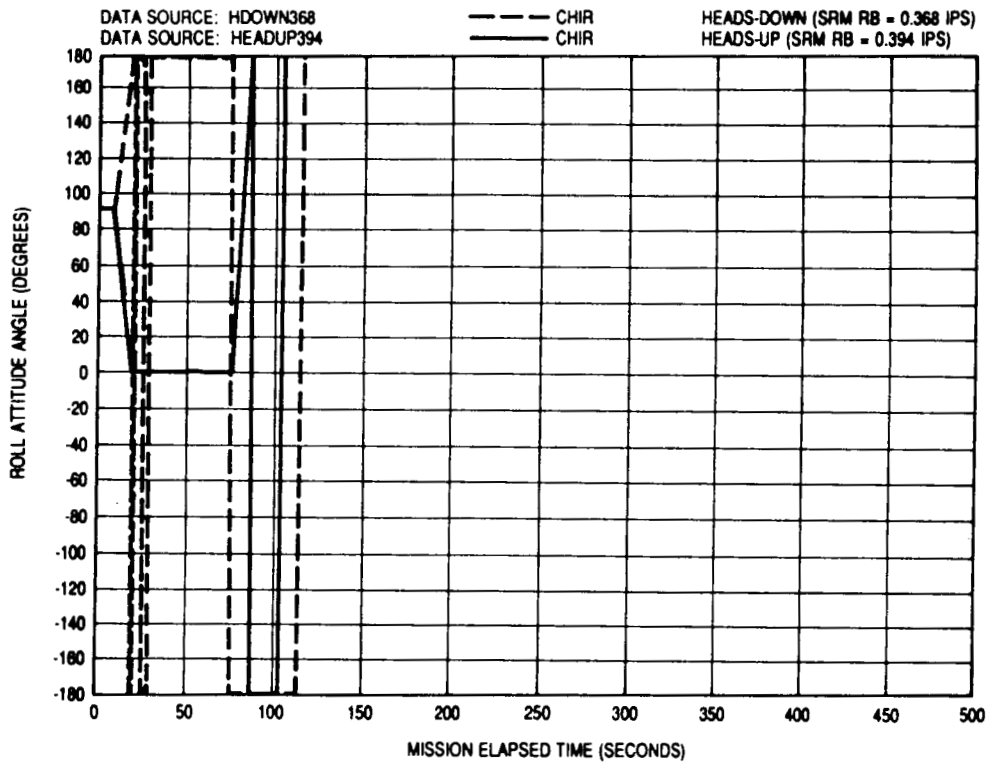


Figure 17. Heads-up versus heads-down chi-roll comparison.

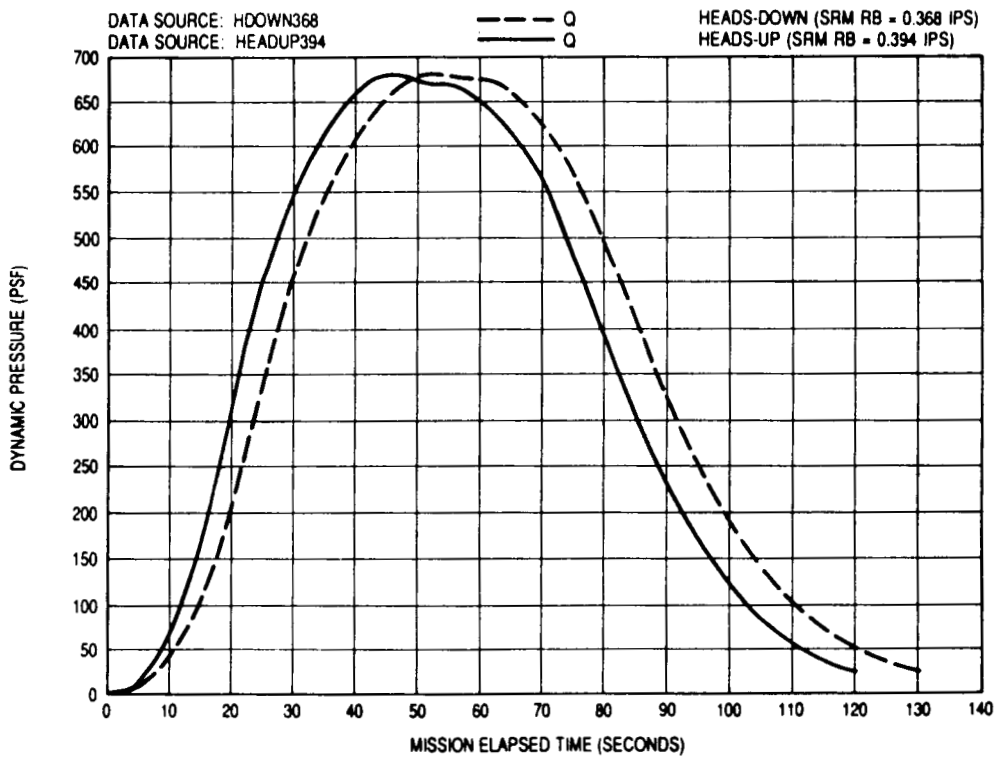


Figure 18. Heads-up versus heads-down Q comparison.

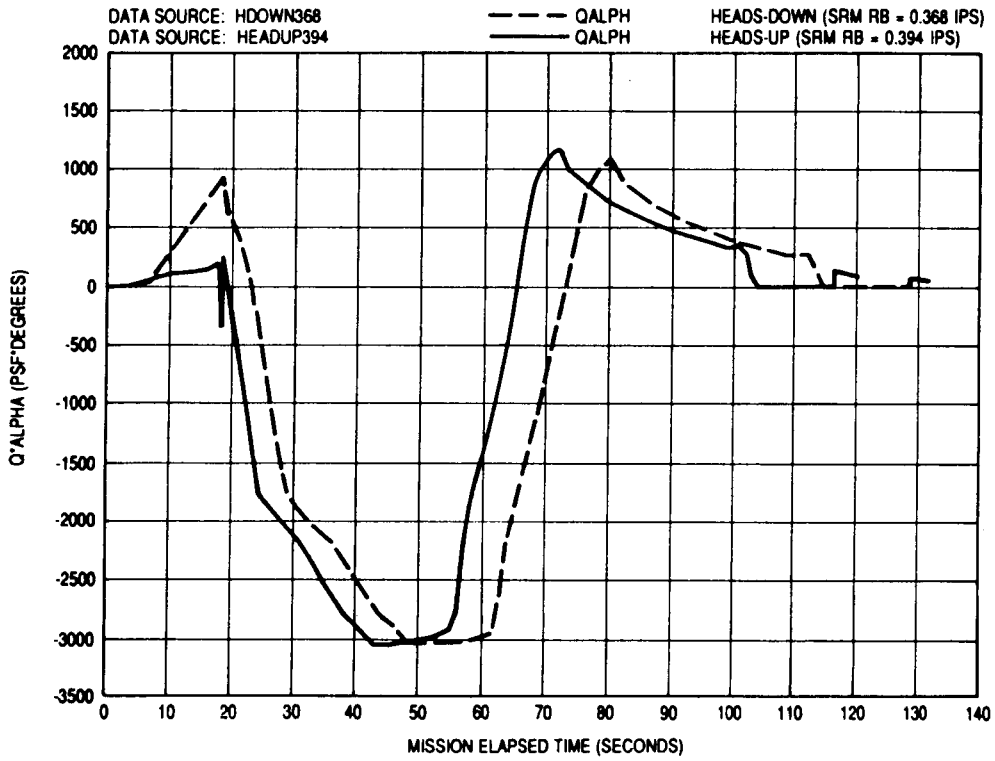


Figure 19. Heads-up versus heads-down Q*alpha comparison.



Figure 20. Heads-up versus heads-down Q*beta comparison.

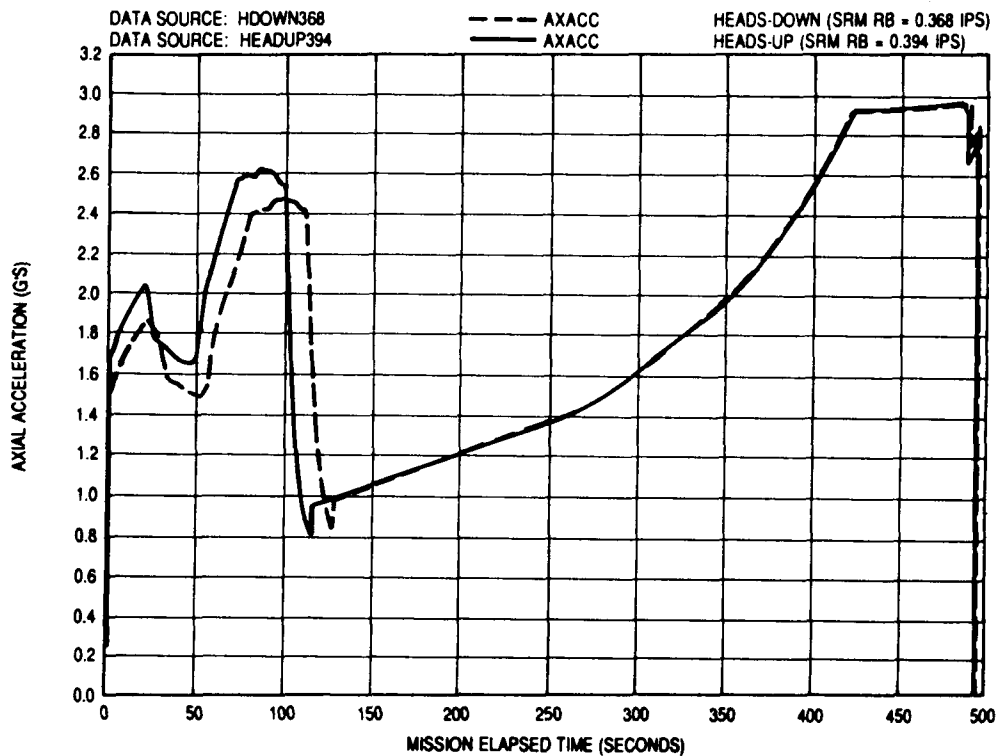


Figure 21. Heads-up versus heads-down acceleration comparison.

IV. DISCUSSION

The evolutionary path of the MASTRE program began with the ROBOT program developed by Dr. R. G. Gottlieb [2]. ROBOT was used to optimize the upper stages of the Saturn rocket series, and since these rockets had symmetric features, a near optimum attitude profile could be attained by the use of a gravity (zero angle of attack) profile. Nonatmospheric optimization algorithms could be used on Saturn upper stages, because its trajectory was significantly out of the atmosphere at both booster cutoff and orbit insertion. However, the airplane-like design and low injection altitude of the Space Shuttle requires the calculation of aerodynamic, atmospheric, asymmetric center of gravity, and thrust effects during the complete ascent flight trajectory. In other words, the STS complexity and trajectory requirements necessitated implementation of atmospheric optimization, along with the additional constraint of thrust vector control moment balance. The Lifting ROBOT program [3], also developed by Dr. Gottlieb, and the RAGMOP program [1], developed by a team assisted by Dr. Gottlieb and Dr. J. T. Lyons, were the first optimization attempts within the atmosphere and STS related constraint enforcement. Features from these programs are incorporated into the current MASTRE program, developed by a team led by Dr. Lyons, along with the additional adjoint equations required by the complex equations of motion of the STS.

The min-H optimization strategy employed by the MASTRE program has proved to be a computationally fast and stable method of determining optimum trajectories. Most simulation cases converged to solutions in seven to twelve iterations; however, convergence problems existed for heads-up trajectories initially. The MASTRE program was written to allow the Space Shuttle to fly in either a heads-down or heads-up mode; but since the heads-down mode is the current flight design, only this option had been vastly

exercised. Essentially, this study is the first time the heads-up option in the MASTRE program required use. Therefore, some minor problems were encountered when first attempting to fly the Shuttle heads-up. Some of these problems included: (1) verifying that the heads-up option flag was indeed causing a heads-up attitude, (2) determining the correct sign on roll rate so as to cause a 90 deg roll to heads-up instead of a 270 deg roll, (3) determining the cause of errors in the integration subroutine, and (4) selecting initial estimates of the control parameters which would allow the program to converge to a solution. Once these problems were solved, a heads-up attitude could be flown from the start of the pitchover phase through MECO. However, recall that a 180 deg roll to heads-down prior to SRB jettison, initiated at Mach 2.5, improved the performance of an initially heads-up trajectory. So, a new code was added to the MASTRE program to allow for this second roll maneuver if desired. This modification resulted in the same latter two minor problems stated earlier for an entire heads-up ascent. Note that unless otherwise stated, a heads-up ascent in this study refers to a heads-up attitude from initiation of tiltover until the vehicle achieves a Mach number of 2.5, where a roll maneuver to heads-down is initiated and is maintained thereafter. The problems associated with the additional roll maneuver were eventually solved once proper initial control parameter values were selected. Therefore, the heads-up trajectories were able to converge to an optimum solution.

The results of this study indicate substantial improvements in the STS lift capability can be achieved if heads-up flight is combined with increased SRM ballistic performance. One of the major drivers regulating the amount of increase of STS performance is the maximum Q limit. If Q is unconstrained, then STS lift capability is limited only by propulsion system performance; neglecting vehicle structural, load, and thermal limits. For example, a heads-up trajectory, with 0.398 ips burnrate SRMs and max-Q of 823 psf, increases injection weight by 7847 lbm compared to the baseline heads-down trajectory, with 0.368 ips burnrate SRMs and 680 psf max-Q. However, the dispersed orbiter thermal protection system (TPS) Q limit is 819 psf. Therefore, mission design Q's are nominally around 680 psf in order to provide protection against three sigma system and wind dispersions. So, with Q constrained to this maximum design value, an optimum SRM burnrate of 0.394 ips results for heads-up trajectories. Injection weight is increased by 4293 lbm under these conditions compared to the baseline heads-down ascent. Note that the total injection weight values listed in Tables 1 through 5 do not accurately reflect potential STS performance capability as of this writing. However, the delta injection weight values would be very similar. One reason for the inaccuracy is because an SSME power level of 109 percent RPL was used in all trajectory runs, and this level is currently not to be used except during an abort mode to avoid orbiter ditching. A great deal of testing and analysis needs to be conducted before a 109 percent SSME power level setting is certified for nominal ascent. The other reason for inaccurate injection weights results from the use of FWC SRM's on all trajectories. This type of SRM was under development and testing when this study was initiated. However, due to the STS 51-L (Challenger) accident and the ensuing SRM redesign, development of this motor has been mothballed. Also,, studies are now underway to examine the use of an Advanced SRM (ASRM) on the STS. Additional comments on the ASRM are mentioned later in this discussion.

A heads-up trajectory with 0.368 ips burnrate SRMs, does not offer a performance advantage compared to the baseline heads-down trajectory. Therefore, payload lift capability of the STS is unaffected for heads-up ascent with no increase in SRM ballistic performance. However, SSME throttling is no longer necessary under these circumstances to satisfy a max-Q constraint of 680 psf. In fact, max-Q is only 662 psf for the heads-up ascent with 0.368 ips burnrate SRMs and unconstrained Q. So, during first stage the potential problems associated with SSME hydraulic lock-up at low power levels are eliminated. Note, this trajectory's reduced Q value of 662 psf does not produce significant load advantages, because the $Q\alpha$ profile is essentially unchanged from the baseline heads-down trajectory.

The performance gain achieved with heads-up flight is due to the relationship between optimum SRM burnrate and Q and $Q\alpha$ constraints being modified to accommodate higher SRM burnrates. The change in the relationship occurs because the existing $Q\alpha$ constraint forces heads-up ascents to fly at a higher altitude or become more lofted, relative to a heads-down ascent (Figs. 7 and 9). The higher altitude profile of the heads-up trajectory decreases dynamic pressure, which decreases SSME throttling requirements and allows flight with higher performing SRMs. These SRMs provide the increased impulse necessary to cause a heads-up ascent to be faster, as well as higher, at SRB separation than a heads-down ascent. Therefore, the overall vehicle performance increases due to increased first stage performance.

Although heads-up flight with increased SRM propellant burnrate enhances STS performance, it also poses several potential problems. One of the most significant problems concerns lift-off load increases. Maximum SRM pressure rise rate and maximum SRM thrust rise rate increase with faster propellant burnrates where the larger rise rates result in increased lift-off loads. Heads-up feasibility studies conducted by Rockwell International [6] indicate significant exceedances in lift-off loads for 0.392 ips burnrate motors. This study also revealed slight exceedances in the post high- Q flight regime loads for 0.392 ips burnrate SRMs. Other issues associated with heads-up flight involve initialization load (I-load) updates and onboard computer software additions. According to Reference 6, a detailed flex/rigid body stability analysis is required to determine new I-loads, such that control stability margin is maintained. Also, to accomplish a roll maneuver to heads-down at Mach 2.5, a roll table needs to be added to the onboard general purpose computer (GPC) flight software, along with elevon schedule changes. A final area of concern deals with ascent venting. Compartments in the STS are designed to vent with increasing altitude in order to equalize pressure. The lofted trajectory associated with heads-up flight may require compartment venting to occur faster than the capabilities of the current system. Further analysis is required to determine if ascent venting is indeed a problem. Overall, some of the heads-up issues mentioned are minor and can be resolved; however, the lift-off load exceedance problem indicates SRM propellant burnrate cannot drastically change.

SRM ballistic performance can be increased by several methods besides increasing propellant burnrate. These methods include increasing propellant load, using a different propellant, and/or changing internal grain geometry. Assessment of these options is currently being evaluated under ASRM contracts managed by MSFC. Note, of primary importance in the ASRM studies is to determine methods to increase safety, reliability, and reproducibility of the SRM. Finally, recent studies by Rockwell International [13] show that if the SRM thrust-time trace shape is recontoured and burnrate is maintained at 0.368 ips, a heads-down ascent can improve the STS performance more than the heads-up ascent. Therefore, the heads-up flight mode does not always offer a performance advantage compared to the heads-down mode.

The Space Shuttle is a complex vehicle and any change in one area usually affects many other areas. This study examined potential STS performance enhancements due to heads-up flight, and showed performance improvements are possible. However, the method used to increase STS performance was to increase SRM burnrate, which adversely affected lift-off loads. Further studies are being conducted to determine a boost phase propulsion system design, which improves STS performance without causing significant side-effects to the overall system. Whether the vehicle flies in a heads-up mode or continues to fly in a heads-down mode may well depend on the booster propulsion system it employs.

V. CONCLUSIONS

From the results of this study, the following conclusions can be drawn:

1. Heads-up and heads-down STS ascents can be flown with the same α -Mach number and β -Mach number histories.
2. The optimum SRM propellant burnrate for STS heads-up ascent, with a mission nominal design Q constraint value of 680 psf, is 0.394 ips.
3. Heads-up ascent, with optimum burnrate SRMs and a 680 psf Q constraint, enhances performance by 4293 lbm compared to the baseline heads-down ascent, with 0.368 ips burnrate SRMs and a 680 psf Q constraint.
4. Heads-up ascent employing current target, 0.368 ips, burnrate SRMs does not offer a performance advantage relative to the baseline heads-down ascent. However, SSME throttling for Q control is not necessary in this case, which is advantageous because during first stage the risk of engine hydraulic lock-up at low power levels is eliminated.

REFERENCES

1. Lyons, J. T.; Woltz, W. S.; Abercrombie, G. E.; and Gottlieb, R. G.: Rocket Ascent G-Limited Moment Balanced Optimization Program (RAGMOP). NASA CR-129000, August 1972.
2. Gottlieb, R. G.: ROBOT-Apollo and AAP Preliminary Mission Profile Program, Part I – Mathematical Formulation. NASA CR-61223, May 1968.
3. Gottlieb, R. G.: Lifting ROBOT – Space Shuttle Preliminary Mission Profile Optimization Program. Dynamics Research Corp., Report R-120U, May 29, 1971.
4. Lyons, J. T.: Minimum Hamiltonian Ascent Shuttle Trajectory Evaluation Program (MASTRE) – CLBM Modification. Dynetics, Inc., Technical Report. No. TR-81-MSFC-33803-012, May 1981.
5. Gottlieb, R. G.: Rapid Convergence to Optimum Solutions Using a Min-H Strategy. AIAA J., Vol. 5, No. 2, February 1967.
6. Bellagamba, L.: Heads-Up Flight: A Necessary Step For Significant STS Performance Enhancement. Rockwell International Systems Integration Review Charts, August 19, 1986.
7. Austin, L. D. (data requestor), Shuttle Operational Data Submittal, J-763 Add. 1, NASA-JSC Document.
8. Smith, R. L.: FWC-Cycle III Nominal Ascent Trajectories for an WTR August Launch with 109% SSME P/L (EMS 283-550). Rockwell International Internal Letter No. FSD&P/AFS-85-361, August 22, 1985.
9. MPS Propellant Inventory, STS 61-I Rev. W, August 7, 1985.
10. Cobb, W. A.: MPS Assessment Tag Data For All Flight Engines. Marshall Space Flight Center Memo No. EL24 (86-36), March 3, 1986.
11. Blackwell, D. L.: Heads Up VLS FWC-High Burn Rate Data Submittal. NASA-MSFC Document, April 1, 1985.
12. Bailey, W. R.: STS-2V(62-B) Data Submittal. NASA-MSFC Document, November 7, 1985.
13. Vantino, M. C.: Status of Heads-Up Ascent Trajectory Design with Block II SRB. Rockwell International Systems Integration Review Charts, April 7, 1987.

BIBLIOGRAPHY

Halfman, R. L.: *Dynamics, Volume II, Systems, Variational Methods and Relativity*. Addison-Wesley Publishing Company, Inc., Reading, Massachusetts, 1962.

Hildebrand, F. B.: *Advanced Calculus for Applications*. Second Edition, Prentice-Hall, Inc., Englewood Cliffs, New Jersey, 1976.

Lyons, J. T.: Minimum Hamiltonian Ascent Shuttle Trajectory Evaluation Program (MASTRE) Engineering Manual. Northrop Services, Inc., Technical Report No. TR-275-1628, June 1976.

Millard, S. W.: STS Performance Enhancements for a Heads-Up Ascent Design. AIAA-86-0193, AIAA 24th Aerospace Sciences Meeting, Reno, Nevada, January 6-9, 1986.

APPENDIX
MASTRE NAMELIST INPUT EXAMPLE

ORIGINAL PAGE IS
OF POOR QUALITY

```

1: SRMCASE14*RB304
2: INPUT
3: HEAD=
4: HEAD=
5: HEAD=
6: HEAD=
7: HEAD=
8: CASE=1,
9: LAST=0,
10: MISON= 'NOM
11: NSYST=3*1,2*2,2*4,4*5,
12: HEAD= ' SSME ENG DATA FOR SSME1
13: ENGDAT(1,1)=-30.7887,0.,-0.6393,-16.,0.,470156.,1082.87,4.1234
14: HEAD= ' SSME ENG DATA FOR SSME2
15: ENGDAT(1,2)=-31.2972,-1.3462,-7.0002,-10.,0.,470156.,1082.87,4.1234
16: HEAD= ' SSME ENG DATA FOR SSME3
17: ENGDAT(1,3)=-31.2972,1.3462,-7.0002,-10.,0.,470156.,1082.87,4.1234
18: HEAD= ' SR8 ENG DATA
19: ENGDAT(1,4)=-36.3336,-6.3627,0.,0.,0.,0.,11.3897
20: ENGDAT(1,5)=-36.3336,6.3627,0.,0.,0.,0.,11.3897
21: HEAD= ' OMS ENG DATA
22: ENGDAT(1,6)=-32.5882,-2.2352,-10.8839,-15.817,-6.5,6000.,19.1571.,9406755.
23: ENGDAT(1,7)=-32.5882,2.2352,-10.8839,-15.817,6.5,6000.,19.1571.,9406755.
24: HEAD= ' 4X RCS ENG DATA
25: ENGDAT(1,8)=-33.5100,3.3147,-10.4028,0.,0.,872.,3.0173.,153141,
26: ENGDAT(1,9)=-33.5100,3.3147,-10.4028,0.,0.,872.,3.0173.,153141,
27: ENGDAT(1,10)=-33.5100,-3.3147,-10.4028,0.,0.,872.,3.0173.,153141,
28: ENGDAT(1,11)=-33.5100,-3.3147,-10.4028,0.,0.,872.,3.0173.,153141,
29: TNE(1,1)=3.,2.,4*0.,3.,2.,4*0.,3.,5*0.,3.,5*0.,
30: TNE(1,5)=3.,5*0.,3.,5*0.,3.,5*0.,3.,5*0.,3.,5*0.,
31: TNE(1,9)=3.,5*0.,3.,5*0.,
32: HEAD= ' SYSTEM PROPELLANT LOADS
33: PROP=1619599.,2233196.,0.,25064.,7416.,
34: MPSEFLG=2,7*1,4,1,
35: HEAD= ' SSME THROTTLE SCHEDULE
36: TIMMPS = 0.,0.,3.5,4.4,20.0,23.2,47.,50.2,150.,
37: FTBL = 1.0,1.0,1.00,1.00,1.00,.65,.65,1.00,1.00,
38: THROT=9*1.00,.65,
39: GLIM=8*1E+20,3.,
40: HEAD= ' SSME THROTTLE VS ALT CONSTRAINT TABLE
41: TAUALT=0.,762.,1524.,2651.,76,40000.,
42: TAUTBL=.9.,82.,.76.,.65.,.65,
43: IPR=0,
44: TBLPL = 1.00,1.00,.65,
45: TBLISP=452.70,452.36,450.19,
46: HEAD= ' MIXTURE RATIO=6.014
47: RATIO=.857428
48: FOMS=15*0,
49: WDRUMP=15*0.,
50: WDRCS=15*0.,
51: FRC=15*0.,
52: WDRCS=15*0.,
53: TAUT=102.,14.377,4.,130.8,10.,25.,60.,10.,126.,6.,.5*0.,
54: WJET=0.,311896.,13*0,
55: PRINT=2*1.,5*1000.,3*10.,
56: NOEVT=2,8,
57: TTBL=0.,11.0,13*0.,0.,11.0,13*0.,
58: CPTBL=0.,0.60,28*0.,
59: CYTBL=0.,0.60,28*0.,
60: KWTA=3,3,3,3

```

60: >

ORIGINAL PAGE IS
OF POOR QUALITY

61: TOBL= 116.377,252.8,27*0., TOBL(31)=252.8,494.9,27*0.,
62: CPOTBL=64.,80.,27*0., CPOTBL(31)=75.,110.,27*0.,
63: CYOTBL=7.,9.,27*0., CYOTBL(31)=9.,10.,27*0.,
64: IFACT=2,
65: HEAD= MACH VS ALPHA/BETA FOR PRM-4 HPM-FWC WINTER(WTR) TRAJ'
66: TMACH= 0., 11.23, 27.34, 42.58, 64.80, 80.00
67: 1.04, 1.00, 1.21, 1.31, 1.37, 1.53, 1.60, 1.77, 1.97, 2.18,
68: 2.38, 2.40, 2.81, 3.15, 3.48, 3.68, 3.97, 4.10, 4.15, 4.20,
69: TALFP= 4.77, 5.33, 10.50, 10.05, 5.11, 2.11, -2.09, -4.00, -3.82, -4.30,
70: -4.34, -4.51, -4.47, -4.48, -4.47, -4.47, -4.36, -3.14, -1.06, -1.43,
71: 1.50, 2.26, 1.04, 1.81, 1.00, 2.01, 2.17, 2.42, 3.05, 2.54,
72: TBETA= -3.60, -1.00, .45, 1.17, 1.12, 72.12, .65, .07, .07,
73: -.12, 12.08, .03, -.06, -.00, -.10, .11, -.13,
74: -.14, -.12, -.14, -.15, -.07, -.16, -.21, -.17, -.30, -.50,
75: CHRDOT=-7.84,
76: KP=1.0,
77: KY=1.0,
78: TABLE=20*0., SIGTAB=20*0.,
79: IPOLY=20,
80: IHEAD=0,
81: HDMACH=2.5,
82: CHRPHD=15,
83: S=10*240.00018,
84: XLEN=2*32.766,
85: XREF=0.,0.,
86: ZREF=0.,0.,
87: NOBASE=20,
88: CBAXIL=0.,
89: HEAD= FIRST STAGE C G HISTORY -PRM4-FWC-DEC TRAJ'
90: TBDWT= 0., 213653., 468212., 764454., 908464., 1212034., 1414702.,
91: 1633612., 1669003., 2079477., 2277085., 2452026., 2569351.,
92: 2597589., 2688418.,
93: TXCG= -10.99, -10.96, -10.89, -10.68, -10.32, -9.85, -9.31,
94: -8.74, -8.06, -7.37, -6.72, -6.15, -5.94,
95: -6.03, -6.08
96: TZCG= -4.46, -4.49, -5.2, -5.6, -6.0, -6.4, -6.8,
97: -.74, -.80, -.87, -.95, -1.03, -1.12,
98: -1.15, -1.17,
99: HEAD= SECOND STAGE C G HISTORY/RI-PRM4-HPM-FWC -DEC TRAJ'
100: TBDWT(1,2)=0., 78212., 275535., 438838., 602140., 765443.,
101: 928745., 1087817., 1218686., 1220721., 5*0.,
102: TXCG(1,2)= -2.98, -3.47, -4.81, -6.06, -7.52, -9.33,
103: -11.78, -15.44, -19.76, -19.66, 5*0.,
104: TZCG(1,2)= -1.38, -1.46, -1.71, -1.96, -2.20, -2.75,
105: -3.50, -4.66, -6.18, -6.21, 5*0.,
106: IWNUN=24,
107: IATHOS=0,
108: MTHARRA=24,
109: NCHG=0,
110: ALTSIG=14*0.,
111: DTZ=0,
112: TZERO=0.,
113: TLIFT=6.4,
114: TTILT=16.3,
115: TCHIR=6.4,
116: KRDER=5, KRDERB=3,
117: KIND=2, KINDB=2,
118: STEP=2*25.1, 12*4.,
119: BSTEP=3*1.12*4.,
120: ALAT=34.58130,
120:>

```

121: ALONG=120.62528,
122: ALT=182.32,
123: MGLAS=66.25,
124: AZ=191.5,
125: FAZ=270.,
126: JUMP=1,
127: VIV=20*0.,
128: WOI=4450907.,
129: JSTART=5.11,
130: JSTRT=5,
131: JETET=0,
132: LPRINT=0,
133: NCOAST=0,
134: NMAX=20,
135: NTABLE=0,
136: HEAD=' PRM-4 FWC DEC PSEUDO MECO TARGET
137: KCDPHI=1,2,3,4,10,11,
138: PSIREQ=7734.0,65.6483724.,98.,-4.10119,
139: NVRST=2
140: KCDRES(1,1)=15.5*0,0,
141: PSIRST(1,1)=680.,5*0.,0.,
142: KDB=3*0,0,4*0,1,8*0,1,6*0,1,1,1*0,
143: KDB(20)=1,
144: VRINT=2*0,
145: VSLOPE=2*0.,
146: ICONSW=2,
147: FPRFAC=.0085,
148: XJEXT=1,
149: MINH=3,
150: NBGCT=3,5,
151: NENDCT=5,11,
152: NP=11,20,
153: WIBT=15*1.,
154: TIMTAU=4.,
155: NTAU=4,
156: HEAD=' HEADS-UP PRM-4(DEC)/SRM-TC-MD-MAX2-NTR(54 DEG)/FWC/NOM/'
157: $END
EOF:157 SCAN:36
0:>
#OUTPUT INTERRUPT*

```

ORIGINAL PAGE IS
OF POOR QUALITY

APPROVAL

**A STUDY TO EVALUATE STS HEADS-UP ASCENT TRAJECTORY
PERFORMANCE EMPLOYING A MINIMUM-HAMILTONIAN
OPTIMIZATION STRATEGY**

By Sujit Sinha

The information in this report has been reviewed for technical content. Review of any information concerning Department of Defense or nuclear energy activities or programs has been made by the MSFC Security Classification Officer. This report, in its entirety, has been determined to be unclassified.

A handwritten signature in cursive script, reading "J P McCarty", is written over a horizontal line.

JOHN P. McCARTY
Director, Propulsion Laboratory

1. REPORT NO. NASA TP-2793		2. GOVERNMENT ACCESSION NO.		3. RECIPIENT'S CATALOG NO.	
4. TITLE AND SUBTITLE A Study To Evaluate STS Heads-Up Ascent Trajectory Performance Employing a Minimum-Hamiltonian Optimization Strategy				5. REPORT DATE February 1988	
				6. PERFORMING ORGANIZATION CODE	
7. AUTHOR(S) Sujit Sinha				8. PERFORMING ORGANIZATION REPORT #	
9. PERFORMING ORGANIZATION NAME AND ADDRESS George C. Marshall Space Flight Center Marshall Space Flight Center, Alabama 35812				10. WORK UNIT NO. M-580	
				11. CONTRACT OR GRANT NO.	
				13. TYPE OF REPORT & PERIOD COVERED Technical Paper	
12. SPONSORING AGENCY NAME AND ADDRESS National Aeronautics and Space Administration Washington, D.C. 20546				14. SPONSORING AGENCY CODE	
15. SUPPLEMENTARY NOTES Prepared by Performance Analysis Branch, Propulsion Systems Division, Propulsion Laboratory, Science and Engineering Directorate.					
16. ABSTRACT A study was conducted to evaluate the performance implications of heads-up ascent flight design for the Space Transportation System, as compared to the current heads-down flight mode. The procedure involved the use of the Minimum Hamiltonian Ascent Shuttle Trajectory Evaluation program, which is a three-degree-of-freedom moment balance simulation of shuttle ascent. A minimum-Hamiltonian optimization strategy was employed to maximize injection weight as a function of maximum dynamic pressure constraint and Solid Rocket Motor burnrate. Performance Reference Mission Four trajectory groundrules were used in all cases for consistency. The major conclusions are that for heads-up ascent and a mission nominal design maximum dynamic pressure value of 680 psf, the optimum solid motor burnrate is 0.394 ips. This optimum burnrate produces a performance enhancement of 4293 lbm relative to the baseline heads-down ascent, with 0.368 ips burnrate solid motors and a 680 psf dynamic pressure constraint. However, no performance advantage exists for heads-up flight if the current Solid Rocket Motor target burnrate of 0.368 ips is used. The advantage of heads-up ascent flight employing the current burnrate is that Space Shuttle Main Engine throttling for dynamic pressure control is not necessary.					
17. KEY WORDS Ascent Performance Minimum Hamiltonian Heads-Up Ascent SRM Burnrate			18. DISTRIBUTION STATEMENT Unclassified - Unlimited Subject Category 13		
19. SECURITY CLASSIF. (of this report) Unclassified		20. SECURITY CLASSIF. (of this page) Unclassified		21. NO. OF PAGES 53	22. PRICE A04